Newton's disc

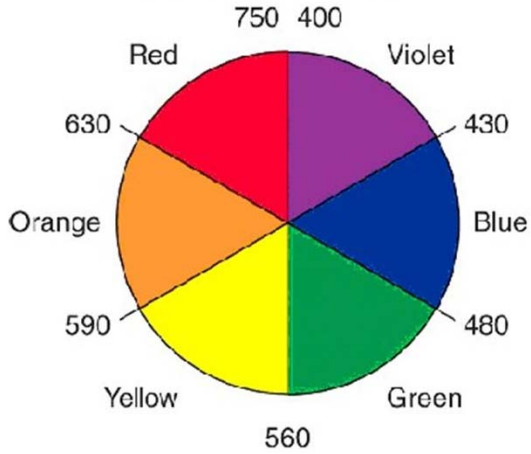

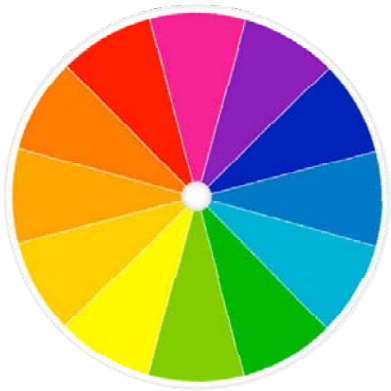

If the Newton's disc is spun quickly, we shall see white

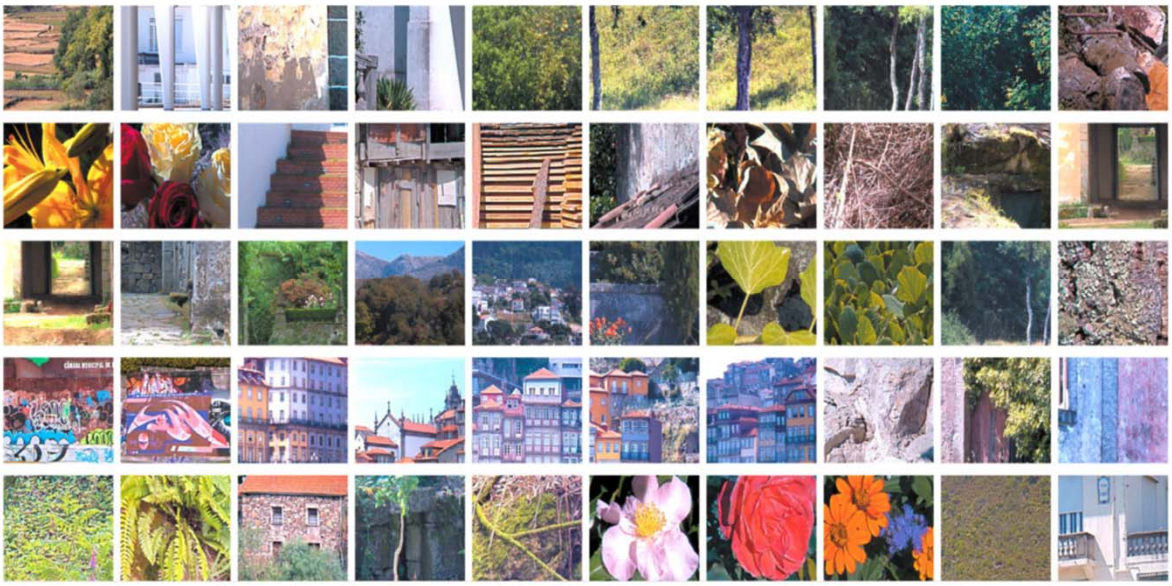

Fig. 1. (Color online) Thumbnails of the 50 scenes analyzed in this study.

Table 1. Estimates Obtained Using the Color-Difference Formula CIEDE2000: Average Number of Discernible Colors for the Set of 50 Scenes Analyzed and Asymptotic Values Obtained from the Exponential Fits

Parameter	(L^*, a^*, b^*)	(a^*, b^*)
Average number of discernible colors	274,736 (92,976)	11,276 (3,232)
Asymptotic values	2,275,698	26,256

Esquema de um espectrofotômetro UV-VIS

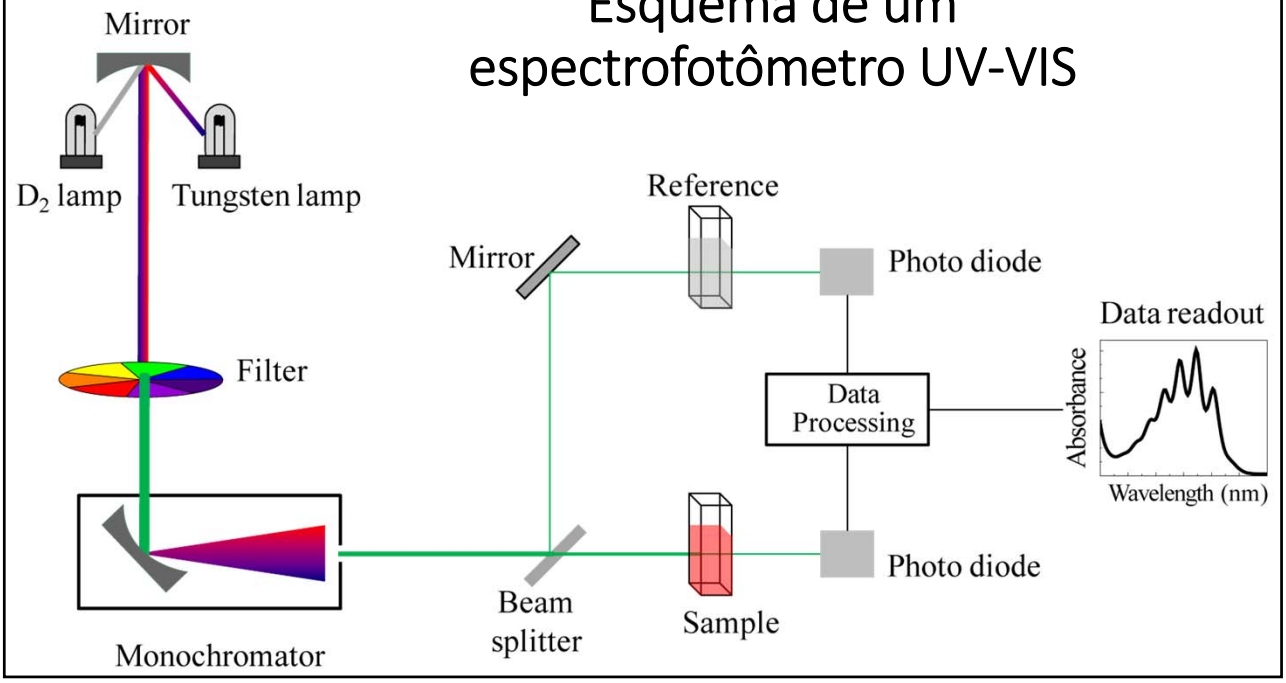

Curva padrão

$$A = \varepsilon c l$$

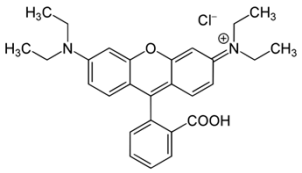

https://en.wikipedia.org/wiki/Rhodamine_B

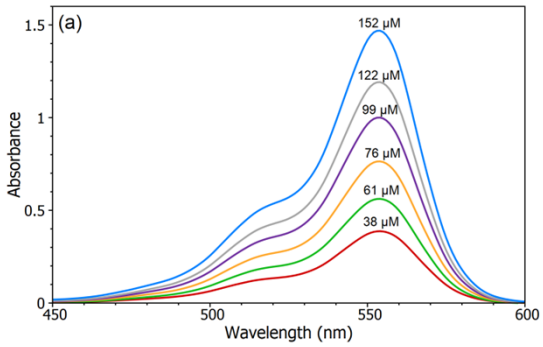

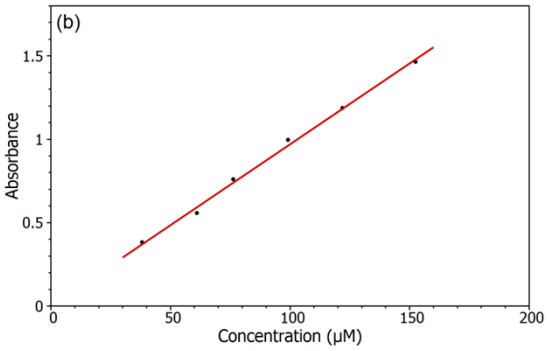

https://www.edinst.com/blog/the-beer-lambert-law/

Espectro de absorção do I_2

(em solução)

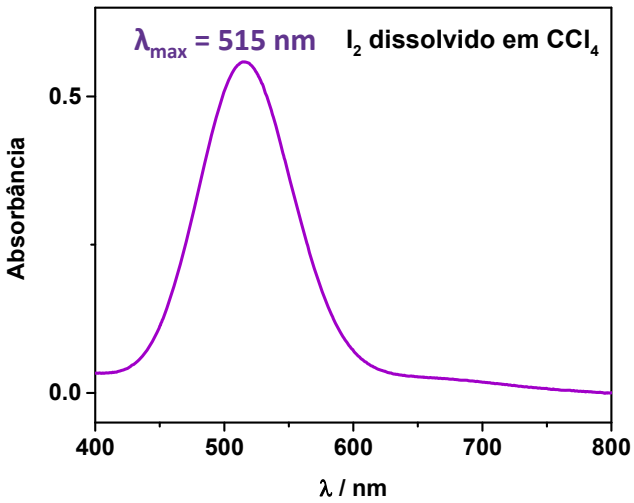

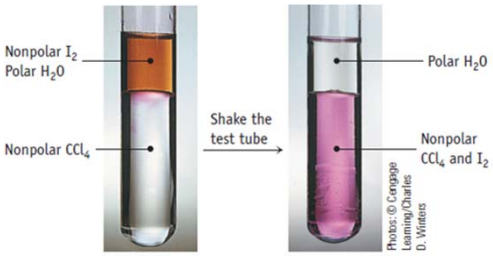

Espectro de absorção do Br_2

(em solução)

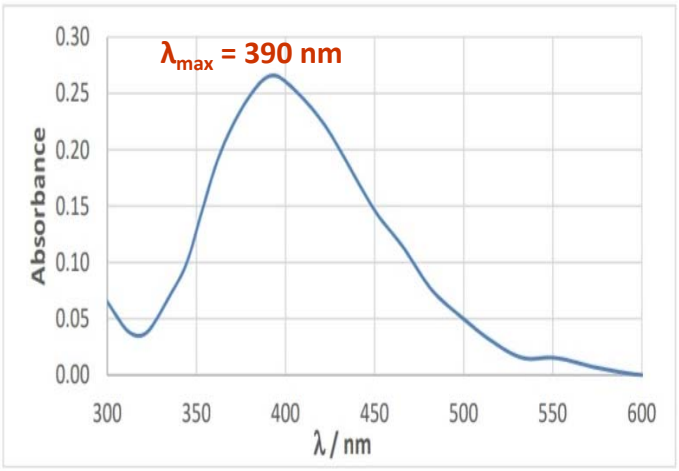

Figure 1: Visible Absorption Spectrum of $Br_2(aq)$

Espectro de absorção do Cl_2

(em solução)

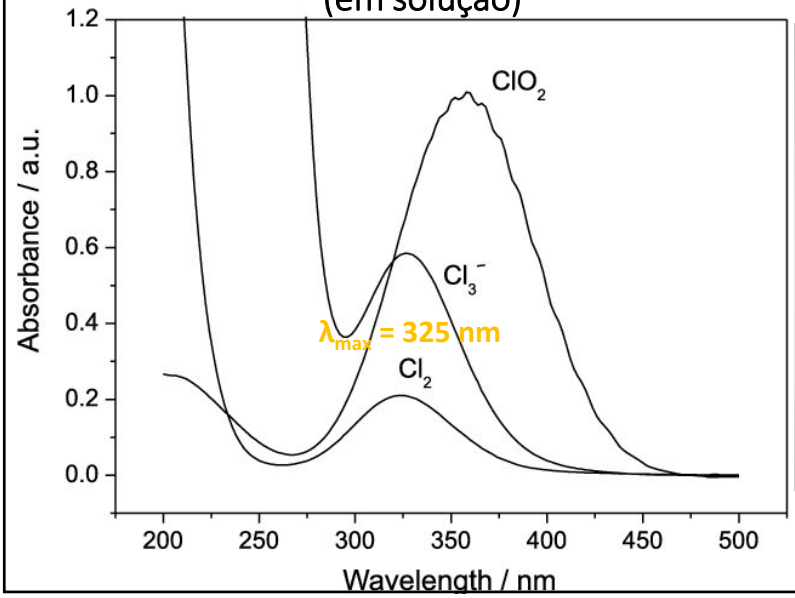

Espectro de absorção do I_2

(em solução)

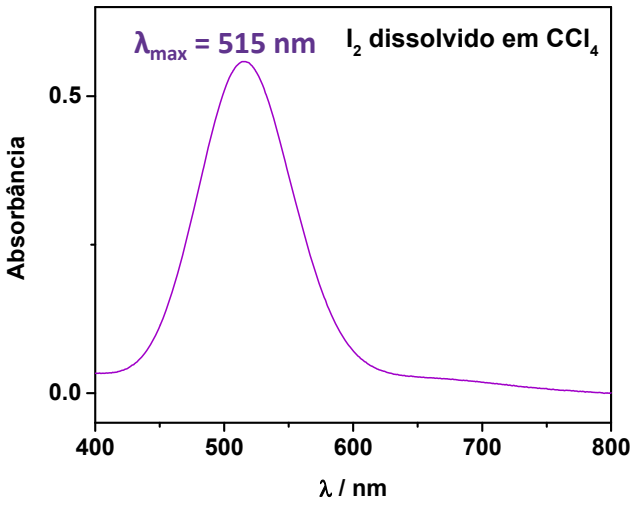

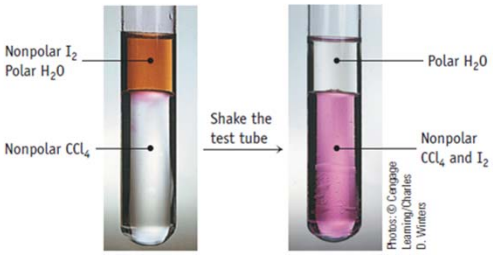

Espectro de absorção do I_2 (vapor)

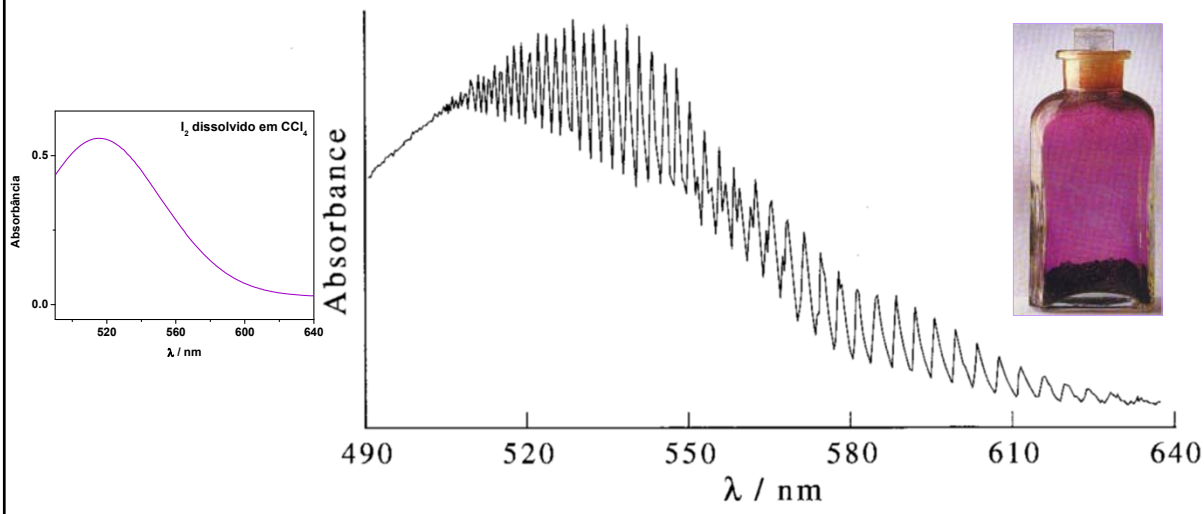

FIGURE 13.9
The absorption spectrum of $I_2(g)$ in the visible region. This spectrum is a v' progression.

Espectro de absorção do I_2 (vapor)

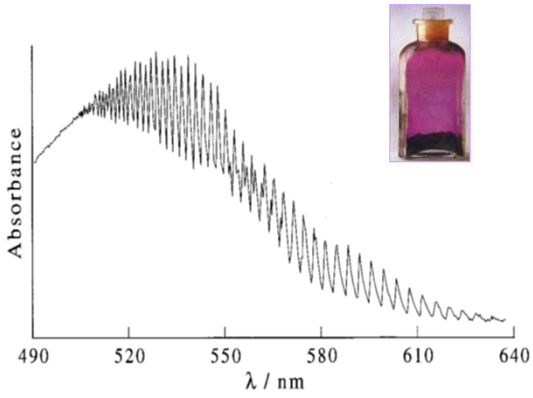

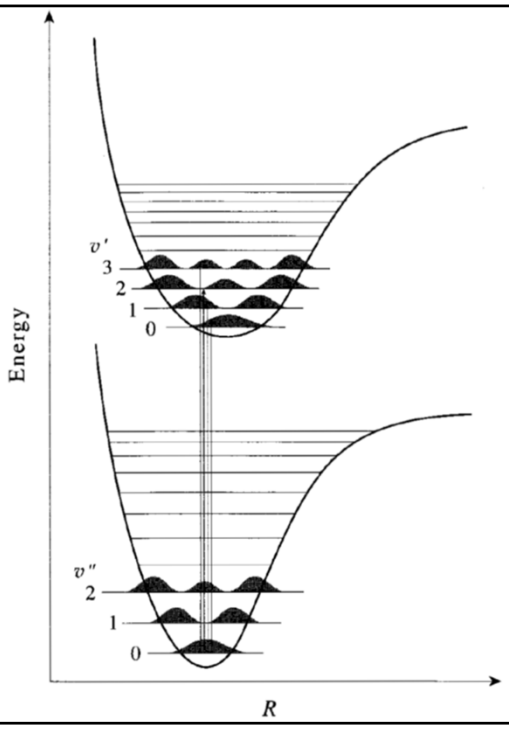

FIGURE 13.9
The absorption spectrum of $I_2(g)$ in the visible region. This spectrum is a v' progression.

Funções de onda – Átomo de 1 elétron

n	ℓ	m_ℓ	Name	Wave Function
				K Shell
1	0	0	$\psi(1s)$	$\frac{1}{\sqrt{\pi}}\left(\frac{Z}{a_0}\right)^{3/2} e^{-\sigma}$
				L Shell
2	0	0	$\psi(2s)$	$\frac{1}{4\sqrt{2\pi}}\left(\frac{Z}{a_0}\right)^{3/2} (2-\sigma)e^{-\sigma/2}$
2	1	0	$\psi(2p_z)$	$\frac{1}{4\sqrt{2\pi}}\left(\frac{Z}{a_0}\right)^{3/2} \sigma e^{-\sigma/2} \cos\theta$
2	1	± 1[b]	$\psi(2p_x)$	$\frac{1}{4\sqrt{2\pi}}\left(\frac{Z}{a_0}\right)^{3/2} \sigma e^{-\sigma/2} \sin\theta \cos\phi$
			$\psi(2p_y)$	$\frac{1}{4\sqrt{2\pi}}\left(\frac{Z}{a_0}\right)^{3/2} \sigma e^{-\sigma/2} \sin\theta \sin\phi$

Funções de onda – Átomo de 1 elétron

M Shell

3	0	0	$\psi(3s)$	$\frac{1}{81\sqrt{3\pi}}\left(\frac{Z}{a_0}\right)^{3/2}(27 - 18\sigma + 2\sigma^2)e^{-\sigma/3}$
3	1	0	$\psi(3p_z)$	$\frac{\sqrt{2}}{81\sqrt{\pi}}\left(\frac{Z}{a_0}\right)^{3/2}(6 - \sigma)e^{-\sigma/3}\cos\theta$
3	1	± 1[b]	$\psi(3p_x)$	$\frac{\sqrt{2}}{81\sqrt{\pi}}\left(\frac{Z}{a_0}\right)^{3/2}(6 - \sigma)\sigma e^{-\sigma/3}\sin\theta\cos\phi$
			$\psi(3p_y)$	$\frac{\sqrt{2}}{81\sqrt{\pi}}\left(\frac{Z}{a_0}\right)^{3/2}(6 - \sigma)\sigma e^{-\sigma/3}\sin\theta\sin\phi$
3	2	0	$\psi(3d_{z^2})$	$\frac{1}{81\sqrt{6\pi}}\left(\frac{Z}{a_0}\right)^{3/2}\sigma^2 e^{-\sigma/3}(3\cos^2\theta - 1)$
3	2	± 1[b]	$\psi(3d_{xz})$	$\frac{\sqrt{2}}{81\sqrt{\pi}}\left(\frac{Z}{a_0}\right)^{3/2}\sigma^2 e^{-\sigma/3}\sin\theta\cos\theta\cos\phi$
			$\psi(3d_{yz})$	$\frac{\sqrt{2}}{81\sqrt{\pi}}\left(\frac{Z}{a_0}\right)^{3/2}\sigma^2 e^{-\sigma/3}\sin\theta\cos\theta\sin\phi$
3	2	± 2[b]	$\psi(3d_{x^2-y^2})$	$\frac{1}{81\sqrt{2\pi}}\left(\frac{Z}{a_0}\right)^{3/2}\sigma^2 e^{-\sigma/3}\sin^2\theta\cos 2\phi$
			$\psi(3d_{xy})$	$\frac{1}{81\sqrt{2\pi}}\left(\frac{Z}{a_0}\right)^{3/2}\sigma^2 e^{-\sigma/3}\sin^2\theta\sin 2\phi$

[a] $\sigma = Zr/a_0$; $a_0 = 4\pi\varepsilon_0\hbar^2/\mu e^2 \simeq 0.5292$ Å

[b] The atomic orbitals having m_ℓ equal to $+1$ or -1 (or $+2$ or -2) are imaginary. The real functions given in this table are linear combinations of those imaginary functions. For example, $2p_x \propto \phi_+ + \phi_-$, where ϕ_+ is the imaginary function having $m_\ell = +1$, and ϕ_- is the imaginary function having $m_\ell = -1$.

Funções de distribuição radial

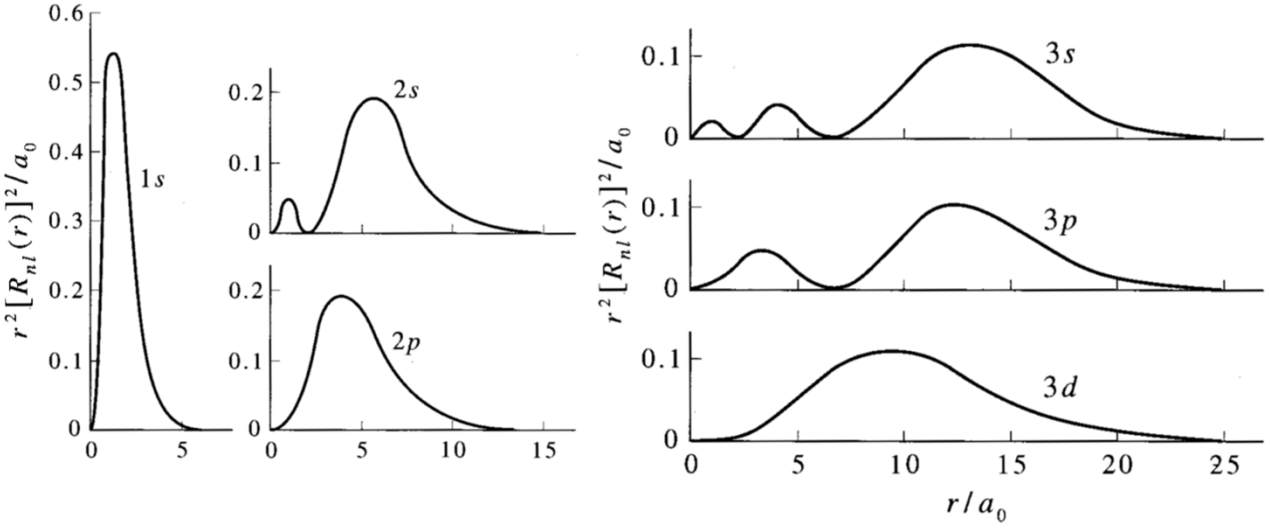

Harmônicos esféricos

l	m_l	$Y_{l,m_l}(\theta,\phi)$
0	0	$\left(\frac{1}{4\pi}\right)^{1/2}$
1	0	$\left(\frac{3}{4\pi}\right)^{1/2}\cos\theta$
	±1	$\mp\left(\frac{3}{8\pi}\right)^{1/2}\sin\theta\,e^{\pm i\phi}$
2	0	$\left(\frac{5}{16\pi}\right)^{1/2}(3\cos^2\theta-1)$
	±1	$\mp\left(\frac{15}{8\pi}\right)^{1/2}\cos\theta\sin\theta\,e^{\pm i\phi}$
	±2	$\left(\frac{15}{32\pi}\right)^{1/2}\sin^2\theta\,e^{\pm 2i\phi}$

l	m_l	$Y_{l,m_l}(\theta,\phi)$
3	0	$\left(\frac{7}{16\pi}\right)^{1/2}(5\cos^3\theta-3\cos\theta)$
	±1	$\mp\left(\frac{21}{64\pi}\right)^{1/2}(5\cos^2\theta-1)\sin\theta\,e^{\pm i\phi}$
	±2	$\left(\frac{105}{32\pi}\right)^{1/2}\sin^2\theta\cos\theta\,e^{\pm 2i\phi}$
	±3	$\mp\left(\frac{35}{64\pi}\right)^{1/2}\sin^3\theta\,e^{\pm 3i\phi}$

The spherical harmonics are orthogonal and normalized in the following sense:

$$\int_0^{\pi}\int_0^{2\pi} Y_{l',m_l'}(\theta,\phi)^* Y_{l,m_l}(\theta,\phi)\sin\theta\,d\theta\,d\phi = \delta_{l'l}\delta_{m_l'm_l}$$

An important 'triple integral' is

$$\int_0^{\pi}\int_0^{2\pi} Y_{l'',m_l''}(\theta,\phi)^* Y_{l',m_l'}(\theta,\phi) Y_{l,m_l}(\theta,\phi)\sin\theta\,d\theta\,d\phi$$

$= 0$ unless $m_l'' = m_l' + m_l$

and we can form a triangle with sides of lengths l'', l', and l (such as 1, 2, and 3 or 1, 1, and 1, but not 1, 2, and 4).

Função de onda completa para o orbital 1s

$$\psi_{1s}(r,\theta,\phi) = R_{10}(r)\,Y_0^0(\theta,\phi) = (\pi a_0^3)^{-1/2} e^{-r/a_0}$$

$$\text{Prob}(1s) = r^2 dr \int_0^{\pi} d\theta\,\sin\theta \int_0^{2\pi} d\phi\,\psi_{1s}^*(r,\theta,\phi)\psi_{1s}(r,\theta,\phi)$$

$$\text{Prob}(1s) = \frac{4}{a_0^3} r^2 e^{-2r/a_0} dr$$

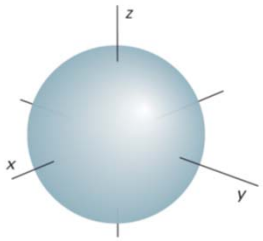

Fig. 9.11 The boundary surface of an s orbital, within which there is a 90 per cent probability of finding the electron.

Orbitais p

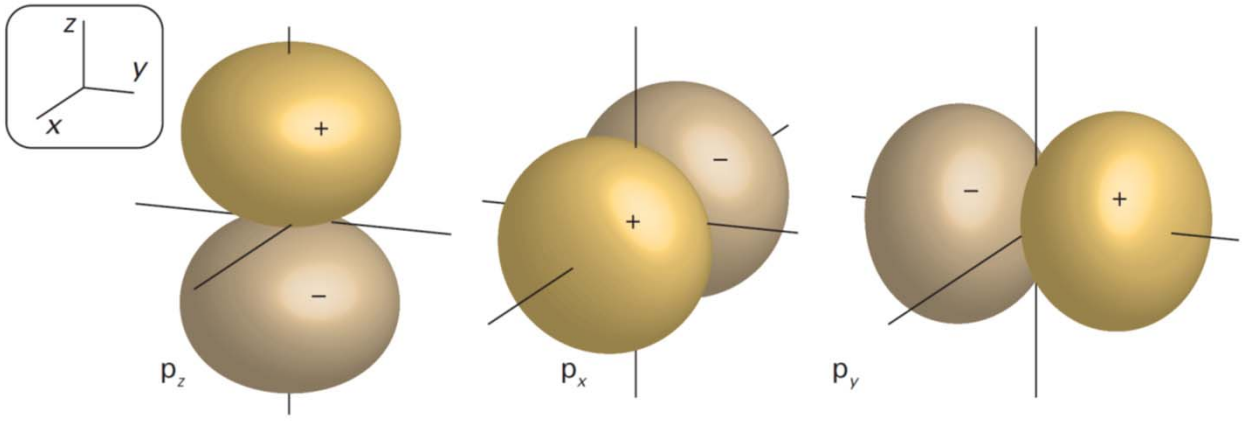

Orbitais d

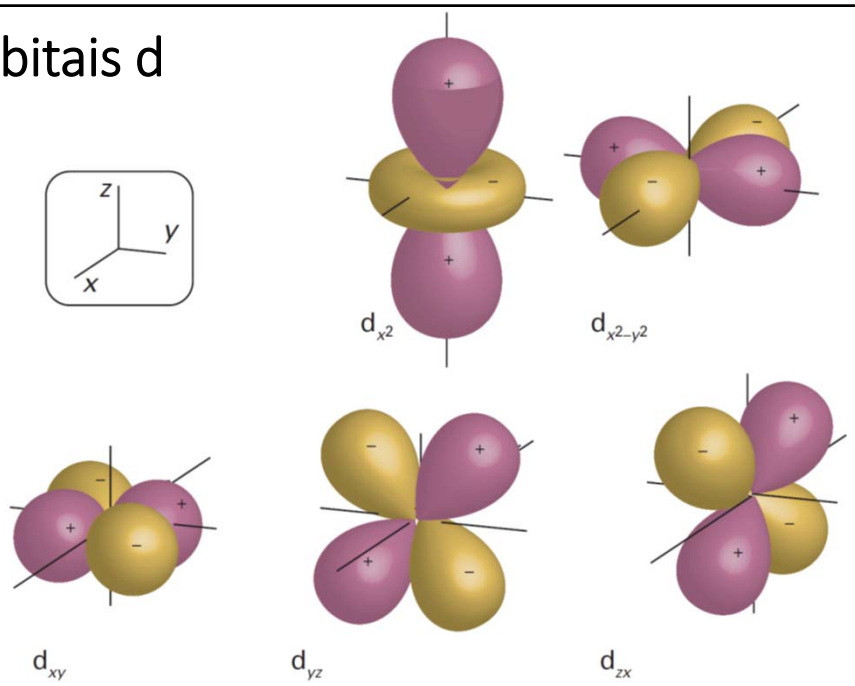

Método variacional

$$E = \frac{\int_{-\infty}^{\infty} \psi^* \mathcal{H} \psi \, d\tau}{\int_{-\infty}^{\infty} \psi^* \psi \, d\tau}$$

Função tentativa: $\psi = c_1 \phi_{1s_A} + c_2 \phi_{1s_B}$

$$1 = \int_{-\infty}^{\infty} (N\psi)^* (N\psi) \, d\tau$$

$$N = (c_1^2 + c_2^2 + 2c_1 c_2 S_{1s_A\ 1s_B})^{-\frac{1}{2}}$$

$$S_{1s_A\ 1s_B} \equiv \int_{-\infty}^{\infty} \phi_{1s_A} \phi_{1s_B} \, d\tau$$

$$E = \int_{-\infty}^{\infty} (N\psi)^* \mathcal{H} (N\psi) d\tau$$

$$= N^2 \int (c_1 \phi_{1s_A} + c_2 \phi_{1s_B}) \mathcal{H} (c_1 \phi_{1s_A} + c_2 \phi_{1s_B}) d\tau$$

$$= N^2 \int (c_1 \phi_{1s_A} + c_2 \phi_{1s_B}) \mathcal{H} (c_1 \phi_{1s_A} + c_2 \phi_{1s_B}) d\tau$$

$$= N^2 [c_1^2 \underbrace{\int \phi_{1s_A} \mathcal{H} \phi_{1s_A} d\tau}_{H_{AA}} + c_1 c_2 \underbrace{\int \phi_{1s_A} \mathcal{H} \phi_{1s_B} d\tau}_{H_{AB}}$$

$$+ c_2 c_1 \underbrace{\int \phi_{1s_B} \mathcal{H} \phi_{1s_A} d\tau}_{H_{BA}} + c_2^2 \underbrace{\int \phi_{1s_B} \mathcal{H} \phi_{1s_B} d\tau}_{H_{BB}}]$$

$$E = N^2[c_1^2 H_{AA} + c_1 c_2 H_{AB} + c_2 c_1 H_{BA} + c_2^2 H_{BB}]$$

$$E = \frac{c_1^2 H_{AA} + c_2^2 H_{BB} + 2c_1 c_2 H_{AB}}{c_1^2 + c_2^2 + 2c_1 c_2 S}$$

$$E(c_1^2 + c_2^2 + 2c_1 c_2 S) = c_1^2 H_{AA} + c_2^2 H_{BB} + 2c_1 c_2 H_{AB}$$

$$\frac{\partial E}{\partial c_1}(c_1^2 + c_2^2 + 2c_1 c_2 S) + E(2c_1 + 2c_2 S) = 2c_1 H_{AA} + 2c_2 H_{AB}$$

$$\frac{\partial E}{\partial c_2}(c_1^2 + c_2^2 + 2c_1 c_2 S) + E(2c_2 + 2c_1 S) = 2c_2 H_{BB} + 2c_1 H_{AB}$$

$$c_1(H_{AA} - E) + c_2(H_{AB} - ES) = 0$$

$$c_1(H_{AB} - ES) + c_2(H_{BB} - E) = 0$$

$$\begin{vmatrix} H_{AA} - E & H_{AB} - ES \\ H_{AB} - ES & H_{BB} - E \end{vmatrix} = 0$$

$$E = \frac{H_{AA} \pm H_{AB}}{1 \pm S}$$

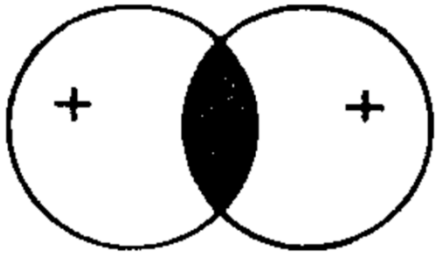

positive overlap

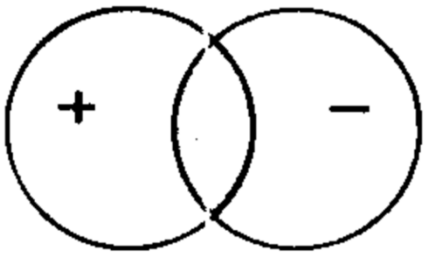

negative overlap

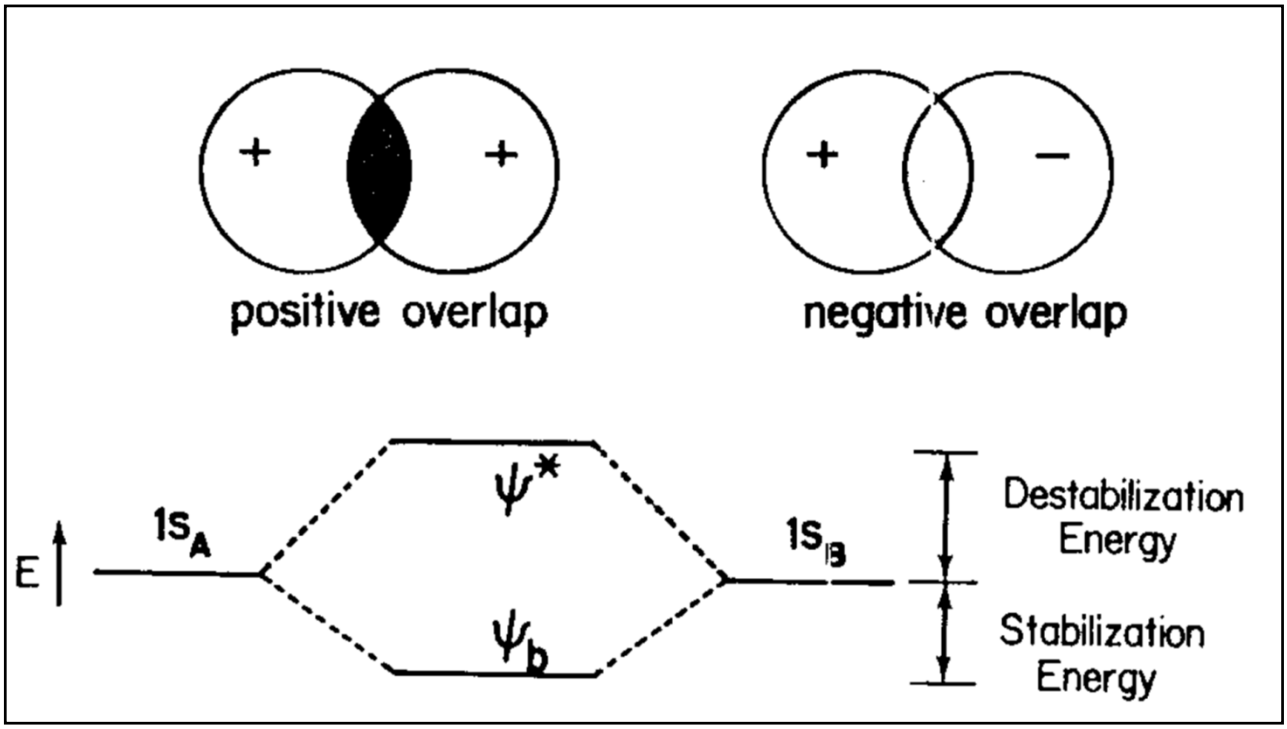

$$\psi^* = \frac{1}{\sqrt{2-2S}}(\phi_{1s_A} - \phi_{1s_B})$$

$$\psi_b = \frac{1}{\sqrt{2+2S}}(\phi_{1s_A} + \phi_{1s_B})$$

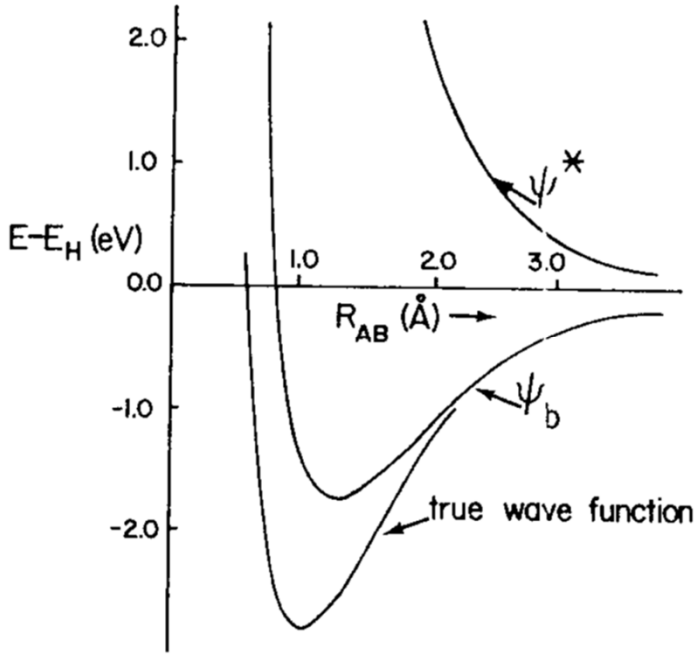

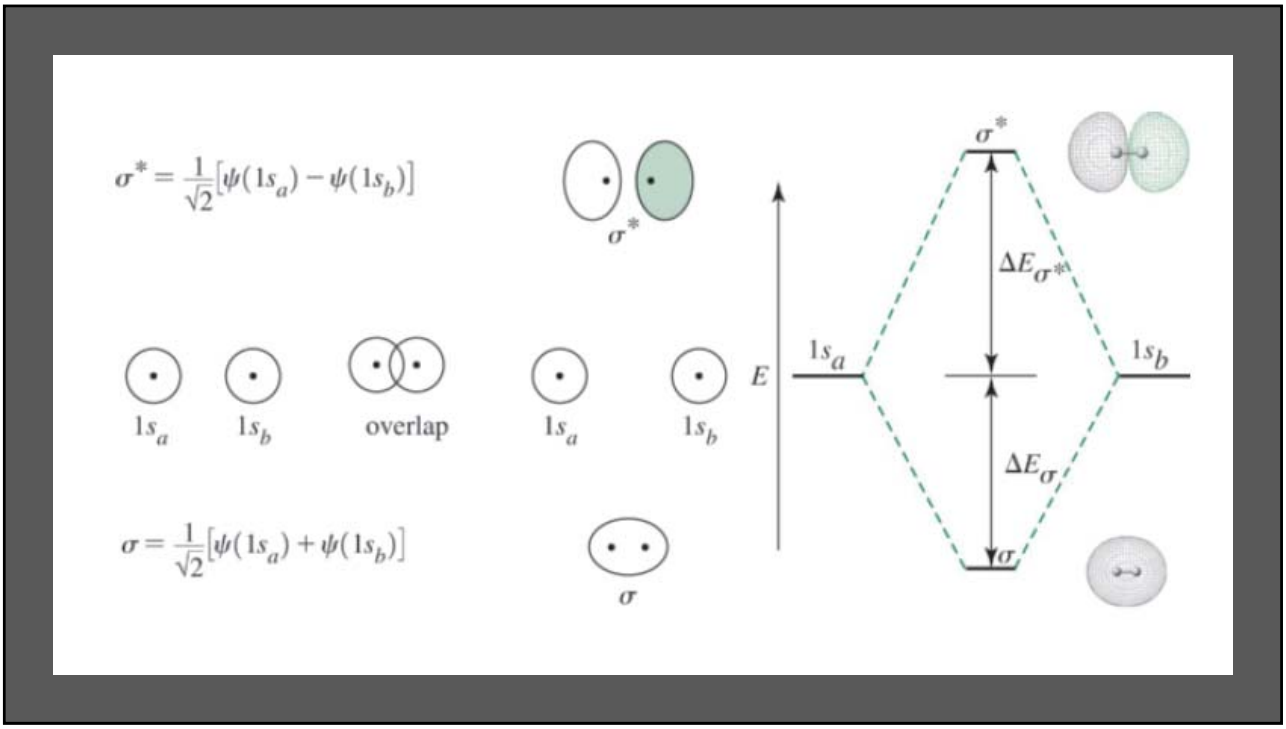

$D_{\infty h}$	E	$2C_\infty^\phi$	$\infty\sigma_v$	i	$2S_\infty^\phi$	∞C_2	
Γ (ls)	2	2	2	0	0	0	$= \sigma_g^+ + \sigma_u^+$

$D_{\infty h}$	E	$2C_\infty^\phi$	$\infty\sigma_v$	i	$2S_\infty^\phi$	∞C_2	
ψ_b	1	1	1	1	1	1	$= \sigma_g^+$
ψ^*	1	1	1	−1	−1	−1	$= \sigma_u^+$

$D_{\infty h}$	E	$2C_\infty^{\phi}$	$\infty\sigma_v$	i	$2S_\infty^{\phi}$	∞C_2	
ψ_b	1	1	1	1	1	1	$= \sigma_g^+$
ψ^*	1	1	1	−1	−1	−1	$= \sigma_u^+$

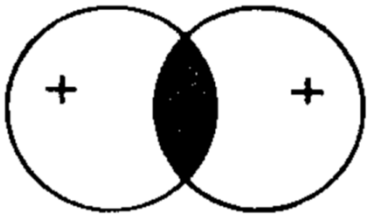

positive overlap

σ_g^+

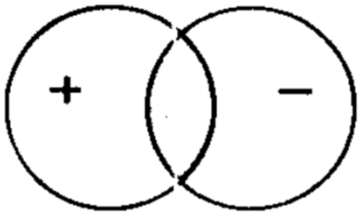

negative overlap

σ_u^+

Sobreposição apenas de orbitais atômicos de mesma simetria

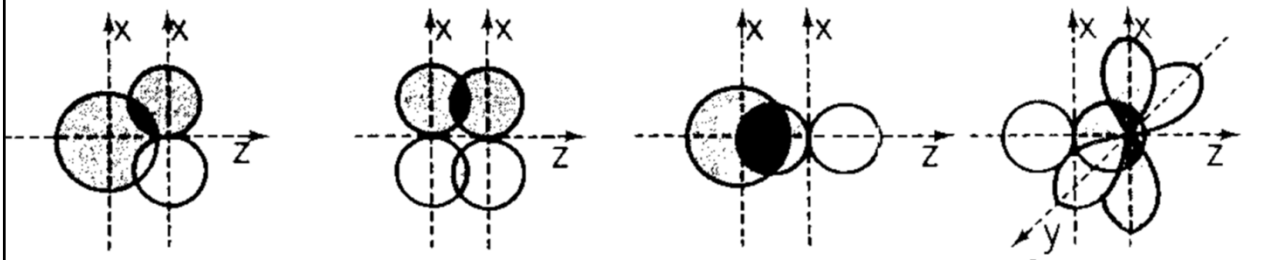

$S_{sp_x} = 0$ $S_{p_x p_x} \neq 0$ $S_{sp_z} \neq 0$ $S_{p_z d_{x^2-y^2}} = 0$

Combinação de orbitais p

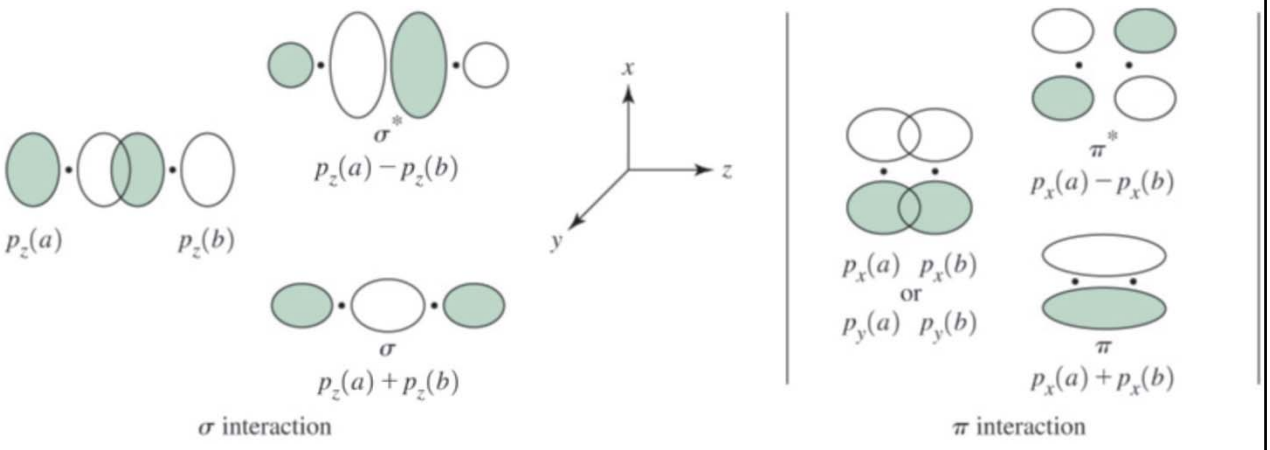

Combinação de orbitais p

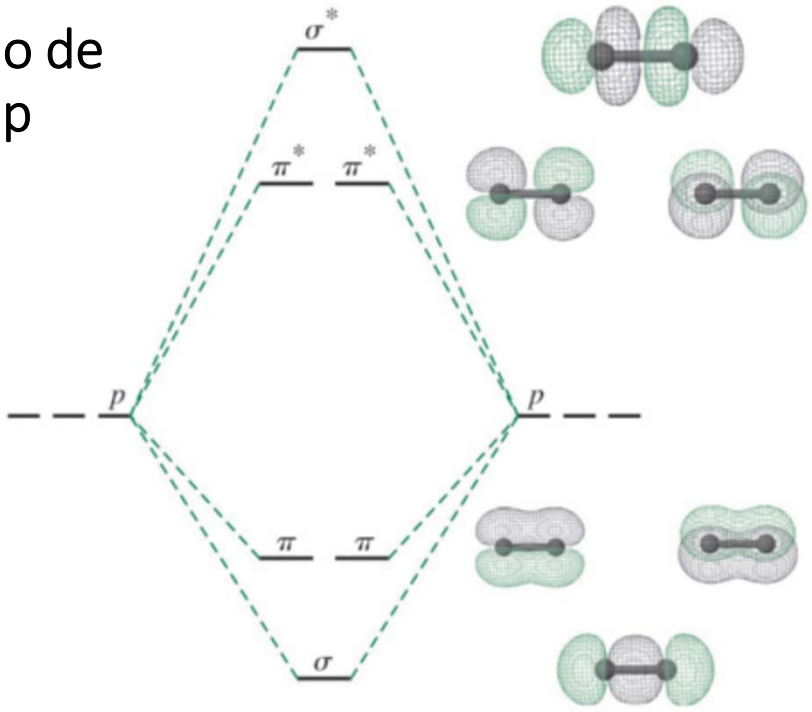

$K = h\nu - IE$

		Orbital Potential Energy (eV)		
Atomic Number	Element	1*s*	2*s*	2*p*
1	H	−13.61		
2	He	−24.59		
3	Li		−5.39	
4	Be		−9.32	
5	B		−14.05	−8.30
6	C		−19.43	−10.66
7	N		−25.56	−13.18
8	O		−32.38	−15.85
9	F		−40.17	−18.65
10	Ne		−48.47	−21.59

Combinação de orbitais para os 10 primeiros elementos

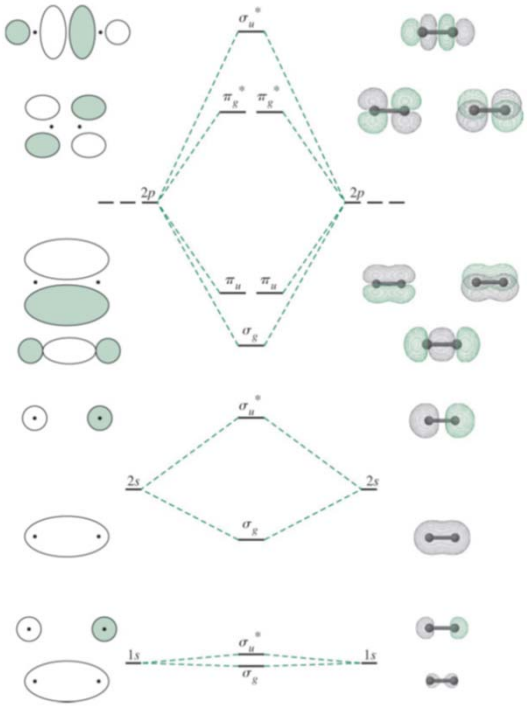

Interação entre orbitais de mesma simetria

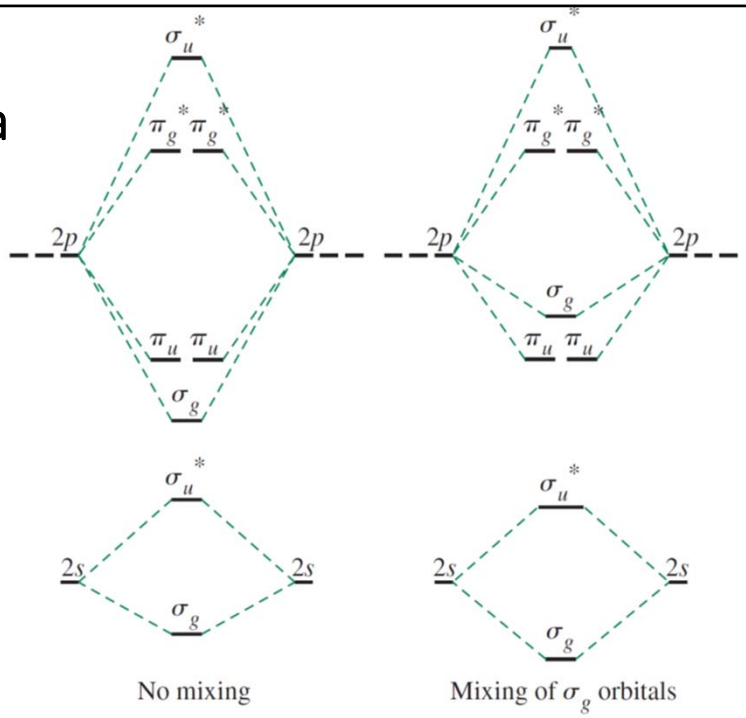

Níveis de energia para moléculas diatômicas homonucleares do segundo período

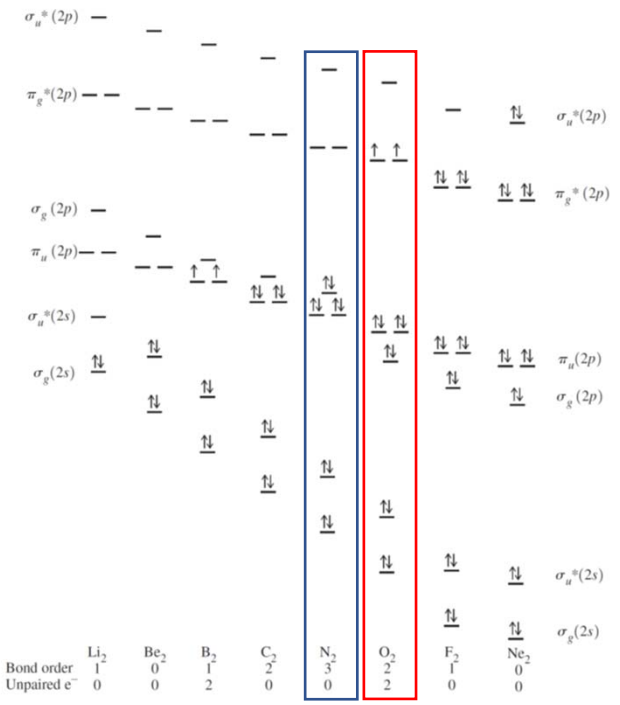

Combinação de orbitais p

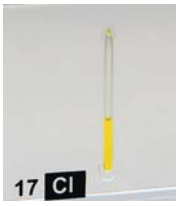

Cl_2

Br_2

I_2

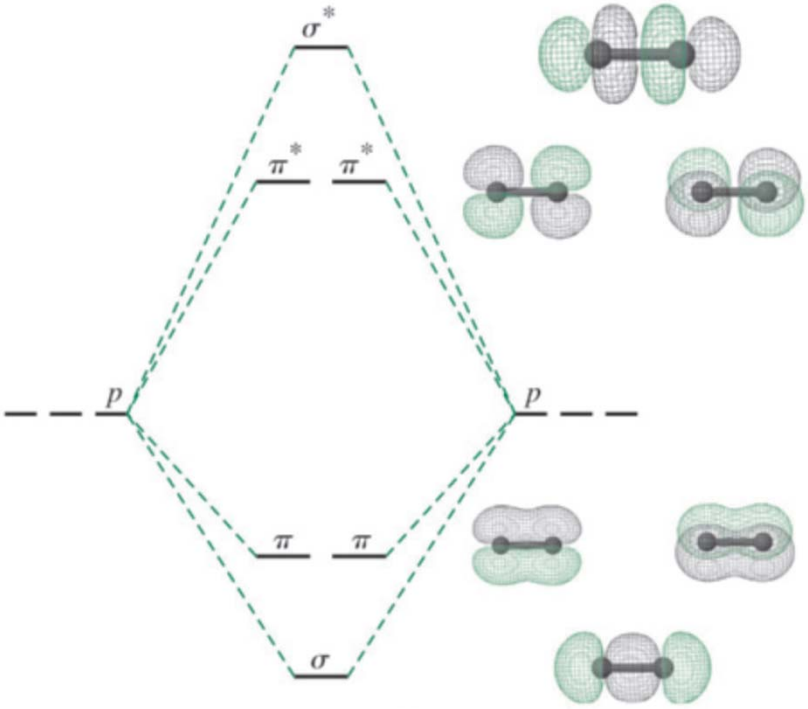

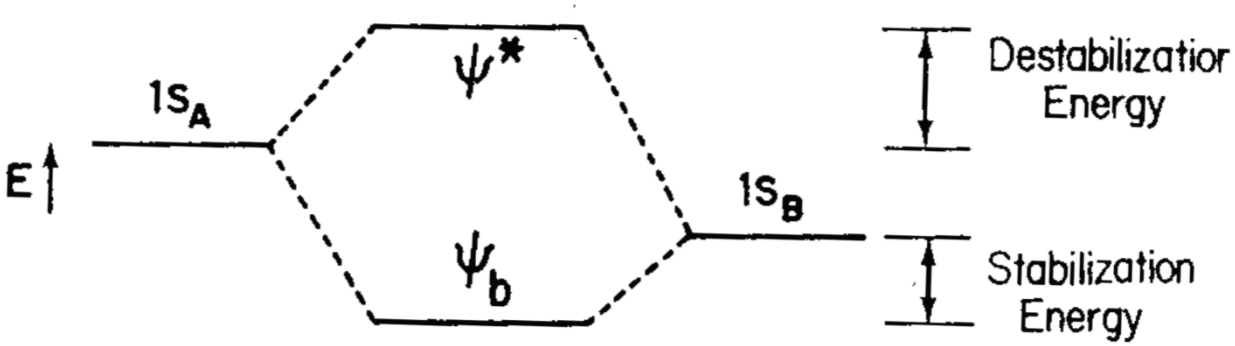

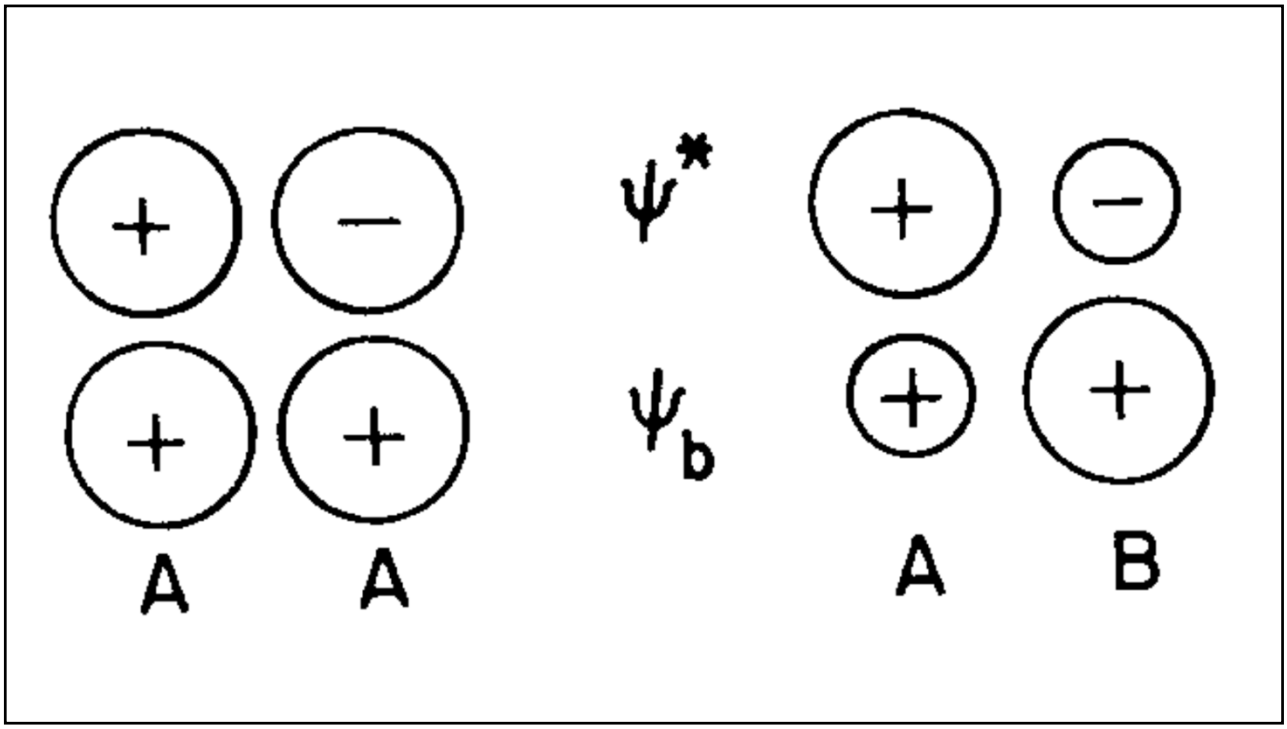

HF

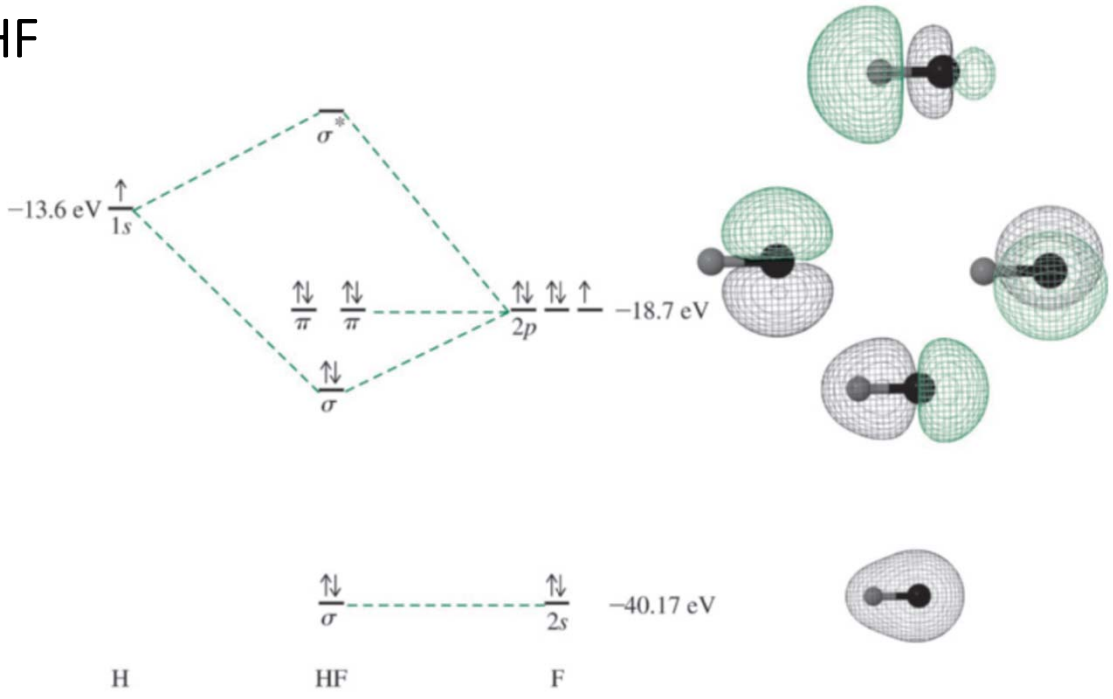

LiF

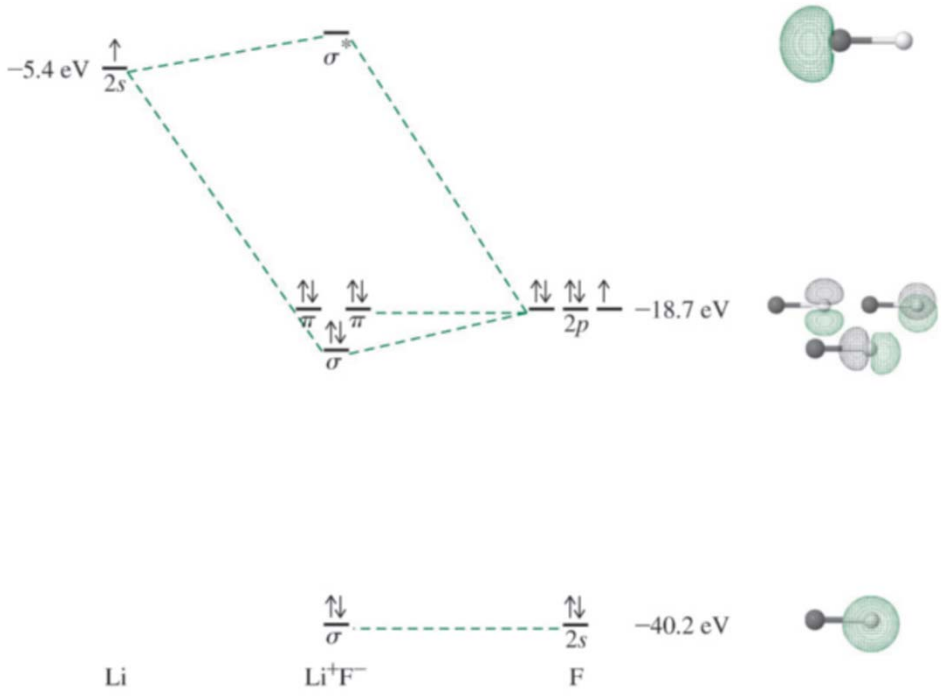

H_2O

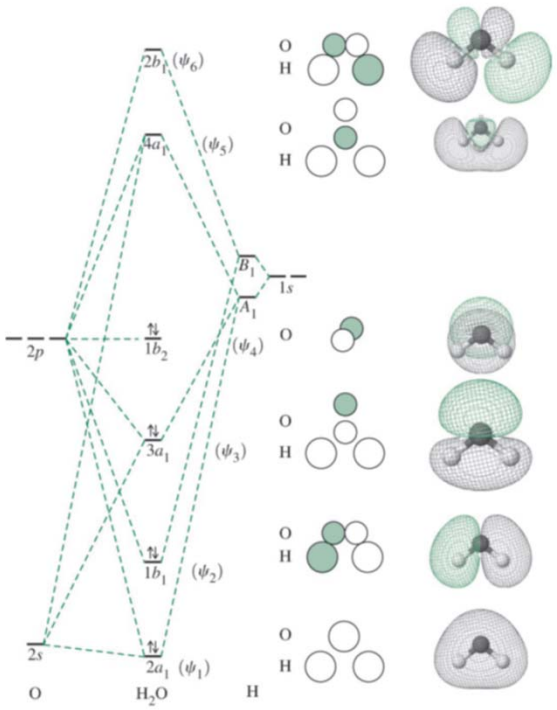

Obs: a notação do Miessler inverte x e y em relação à notação utilizada em aula

3. **Reducible Representations for Outer Atom Orbitals:** In CO_2 these are the $2s$ and $2p$ oxygen orbitals. These can be grouped into four sets (Figure 5.18). For example, the pair of $2s$ orbitals on the oxygen atoms has the following representation:

D_{2h}	E	$C_2(z)$	$C_2(y)$	$C_2(x)$	i	$\sigma(xy)$	$\sigma(xz)$	$\sigma(yz)$
$\Gamma(2s)$	2	2	0	0	0	0	2	2

The other group orbitals have the following representations:

D_{2h}	E	$C_2(z)$	$C_2(y)$	$C_2(x)$	i	$\sigma(xy)$	$\sigma(xz)$	$\sigma(yz)$
$\Gamma(2p_z)$	2	2	0	0	0	0	2	2
$\Gamma(2p_x)$	2	−2	0	0	0	0	2	−2
$\Gamma(2p_y)$	2	−2	0	0	0	0	−2	2

4. **Group Orbitals from Reducible Representations:** Each of the representations from Step 3 can be reduced by the procedure described in Section 4.4.2. For example, the representation $\Gamma(2s)$ reduces to $A_g + B_{1u}$:

D_{2h}	E	$C_2(z)$	$C_2(y)$	$C_2(x)$	i	$\sigma(xy)$	$\sigma(xz)$	$\sigma(yz)$
A_g	1	1	1	1	1	1	1	1
B_{1u}	1	1	−1	−1	−1	−1	1	1

When this procedure is conducted for each representation, the representations describe the symmetry properties of the oxygen atom group orbitals for CO_2, shown with the appropriate D_{2h} labels in Figure 5.18. Note that these group orbitals are the same as those deduced by inspection for the fluorine atoms in FHF^-.

FIGURE 5.18 Group Orbital Symmetry in CO_2.

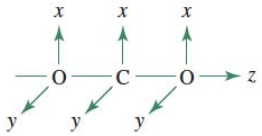

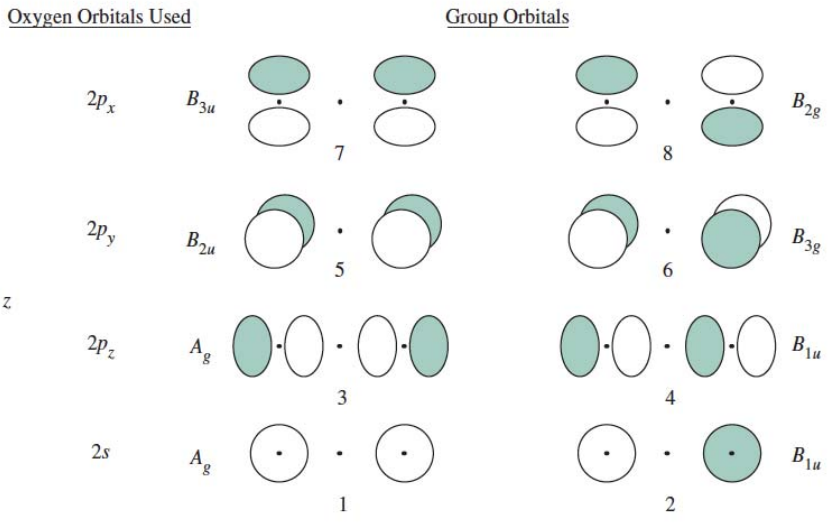

CO_2

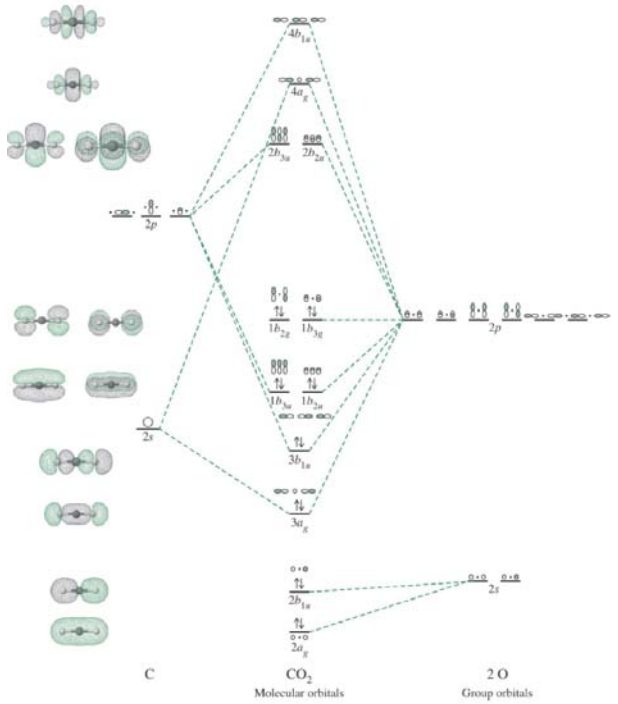

Molecular Orbital Picture of the π Bonding in Benzene

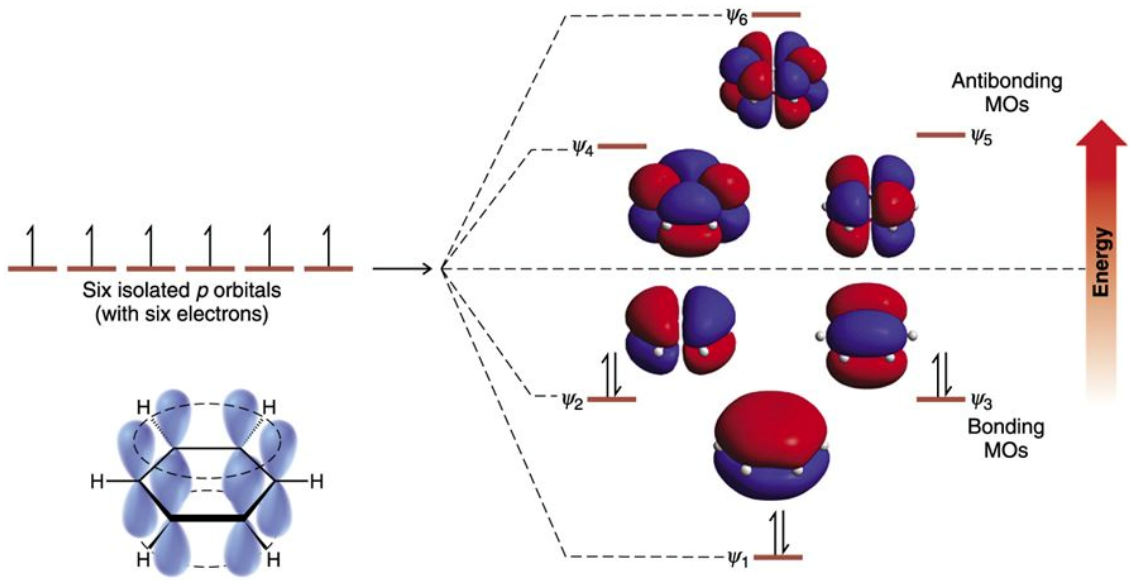

Diagrama de energia – H_2

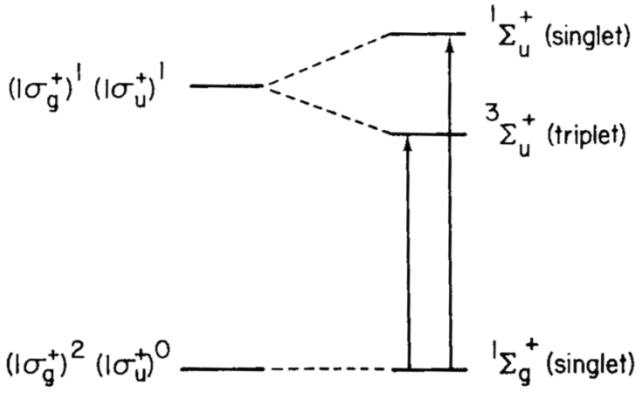

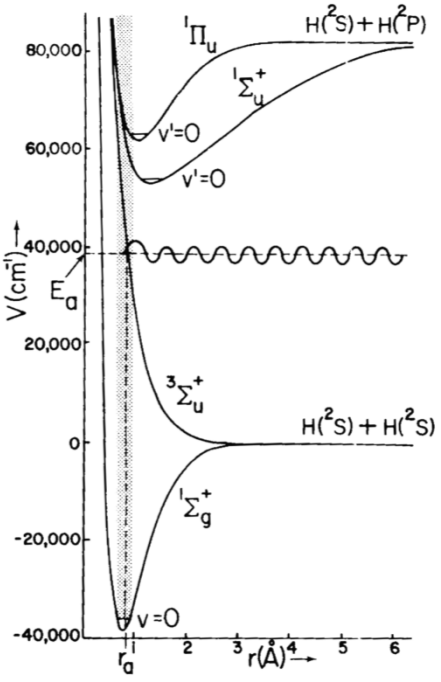

Fator de Franck-Condon

$$\int \psi^*_{v'} \psi_v d\tau_n$$

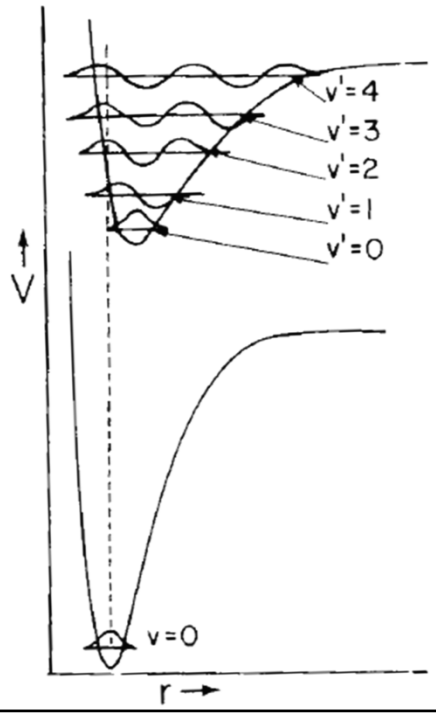

Regra de seleção de orbital

$$\int \psi_e^* \hat{\mu}_e \psi_e d\tau_e$$

Regra de seleção de spin

$$\int \psi_s^* \psi_s d\tau_s$$

Regra de seleção completa:

$$M = \int \psi_v^* \psi_v d\tau_n \int \psi_e^* \hat{\mu}_e \psi_e d\tau_e \int \psi_s^* \psi_s d\tau_s$$

Lei de Lambert-Beer

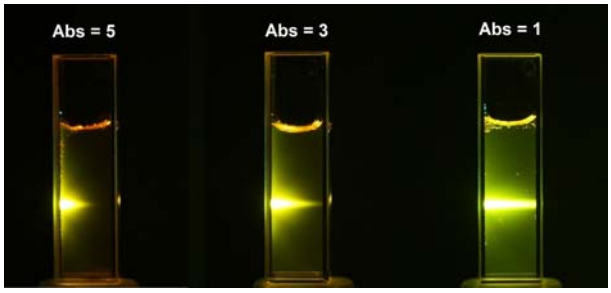

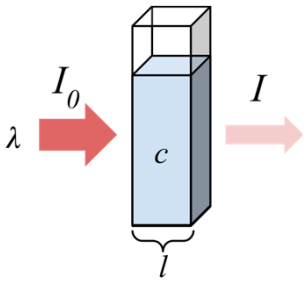

$$T = \frac{I}{I_0} \qquad T(\%) = 100\frac{I}{I_0}$$

$$A = log\frac{I_0}{I} \qquad A = -log\mathrm{T}$$

$$\boldsymbol{A = \varepsilon\, c\, l}$$

A	Absorbância	adimensional
ε	Coef. de absorção molar	$M^{-1}cm^{-1}$
c	Concentração molar	M
l	Caminho ótico	cm

https://www.edinst.com/blog/the-beer-lambert-law/

Valores da absortividade molar, ε

Condição	Faixa de valores aproximados de ε / M^{-1} cm^{-1}
Proibida por spin	10^{-5} a 10^{0}
Permitida por spin, proibida por orbital	10^{0} a 10^{3}
Permitida por spin e por orbital	10^{3} a 10^{5}

$$M = \int \psi_v^* \psi_v d\tau_n \int \psi_e^* \hat{\mu}_e \psi_e d\tau_e \int \psi_s^* \psi_s d\tau_s$$

Molecular Orbital Picture of the π Bonding in Benzene

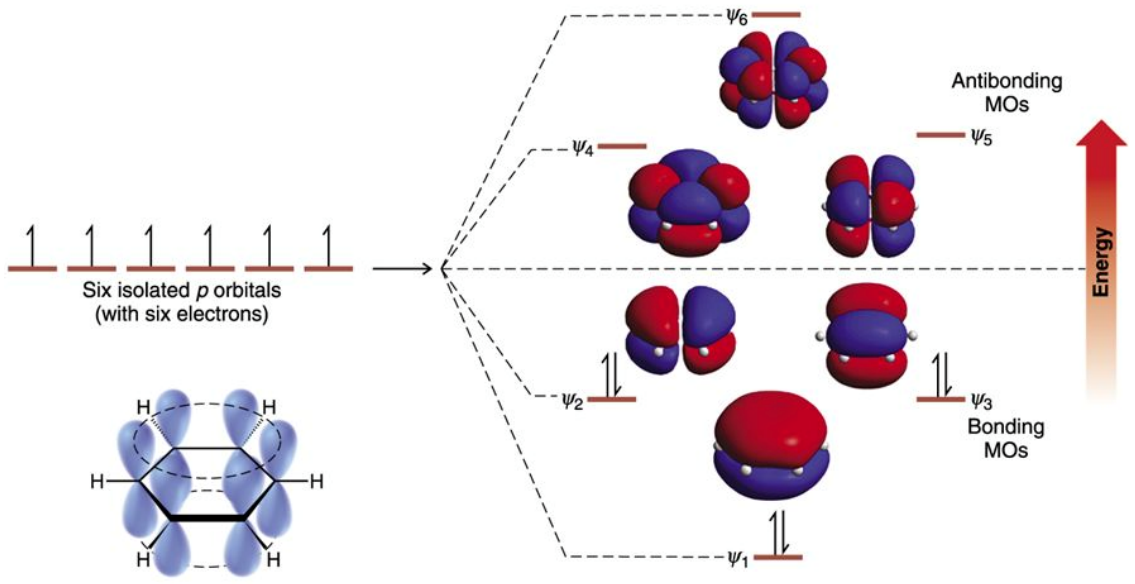

Regra de seleção de orbital

D_{6h}	E	$2C_6$ (z)	$2C_3$	C_2	$3C'_2$	$3C''_2$	i	$2S_3$	$2S_6$	σ_h (xy)	$3\sigma_d$	$3\sigma_v$	linear functions, rotations
A_{1g}	+1	+1	+1	+1	+1	+1	+1	+1	+1	+1	+1	+1	-
A_{2g}	+1	+1	+1	+1	-1	-1	+1	+1	+1	+1	-1	-1	R_z
B_{1g}	+1	-1	+1	-1	+1	-1	+1	-1	+1	-1	+1	-1	-
B_{2g}	+1	-1	+1	-1	-1	+1	+1	-1	+1	-1	-1	+1	-
E_{1g}	+2	+1	-1	-2	0	0	+2	+1	-1	-2	0	0	(R_x, R_y)
E_{2g}	+2	-1	-1	+2	0	0	+2	-1	-1	+2	0	0	-
A_{1u}	+1	+1	+1	+1	+1	+1	-1	-1	-1	-1	-1	-1	-
A_{2u}	+1	+1	+1	+1	-1	-1	-1	-1	-1	-1	+1	+1	z
B_{1u}	+1	-1	+1	-1	+1	-1	-1	+1	-1	+1	-1	+1	-
B_{2u}	+1	-1	+1	-1	-1	+1	-1	+1	-1	+1	+1	-1	-
E_{1u}	+2	+1	-1	-2	0	0	-2	-1	+1	+2	0	0	(x, y)
E_{2u}	+2	-1	-1	+2	0	0	-2	+1	+1	-2	0	0	-

$$\int \psi_e^* \, \hat{\mu}_e \psi_e \, d\tau_e$$

$\Gamma(\psi_e)$ $^1E_{1u} + {}^1B_{2u} + {}^1B_{1u}$

$\Gamma(\mu)$ $A_{2u} + E_{1u}$

$\Gamma(\psi_e)$ $^1A_{1g}$

$A_{2u} \times E_{1u} = 2\ 1\ -1\ -2\ 0\ 0\ 2\ 1\ -1\ -2\ 0\ 0 = E_{1g}$

Regra de seleção de orbital

$E_{1u} \times E_{1u} = 4\ 1\ 1\ 4\ 0\ 0\ 4\ 1\ 1\ 4\ 0\ 0 = \mathbf{A_{1g}} + A_{2g} + E_{2g}$

$B_{2u} \times E_{1u}$ (ou A_{2u}) = ... = $B_{2g} + E_{2g}$

$B_{1u} \times E_{1u}$ (ou A_{2u}) = ... = $B_{1g} + E_{2g}$

Espectro de absorção do benzeno

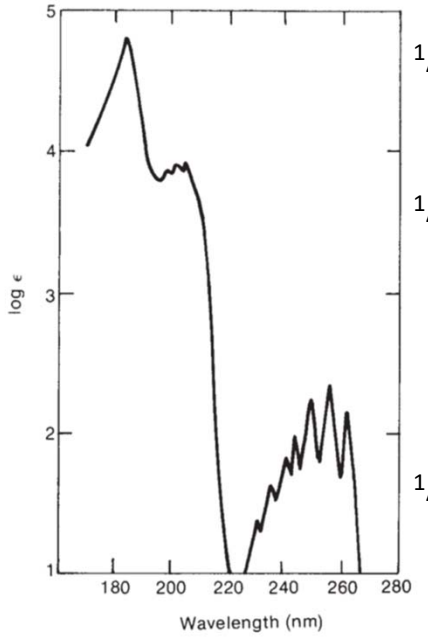

$^1A_{1g} \rightarrow {}^1E_{1u}$ (permitida, ε = 47000)

$^1A_{1g} \rightarrow {}^1B_{1u}$ (proibida, ε = 7400)

$^1A_{1g} \rightarrow {}^1B_{2u}$ (proibida, ε = 230)

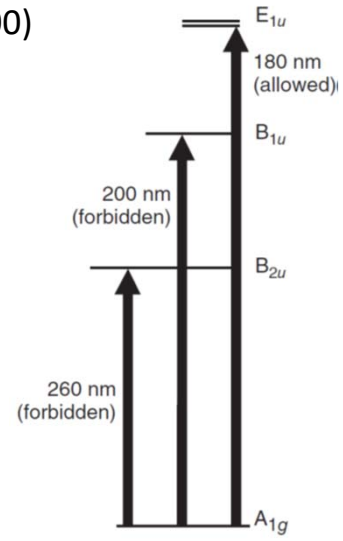

Espectro de absorção do benzeno "na prática"

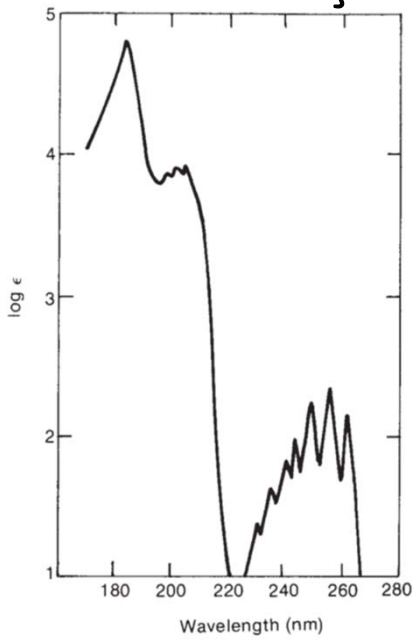

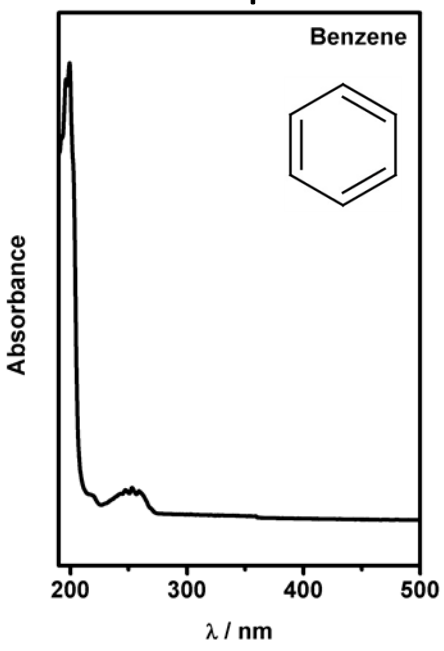

Aromáticos

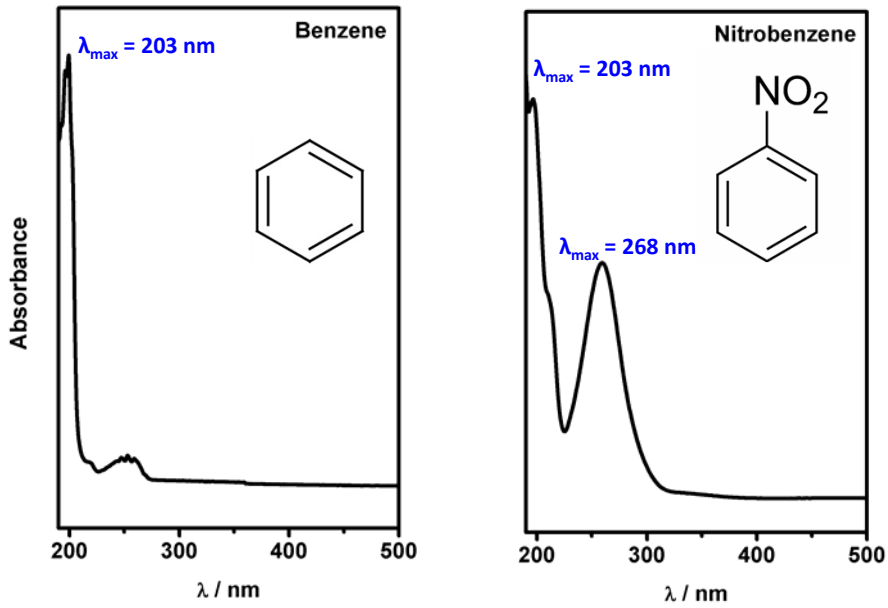

Aromáticos

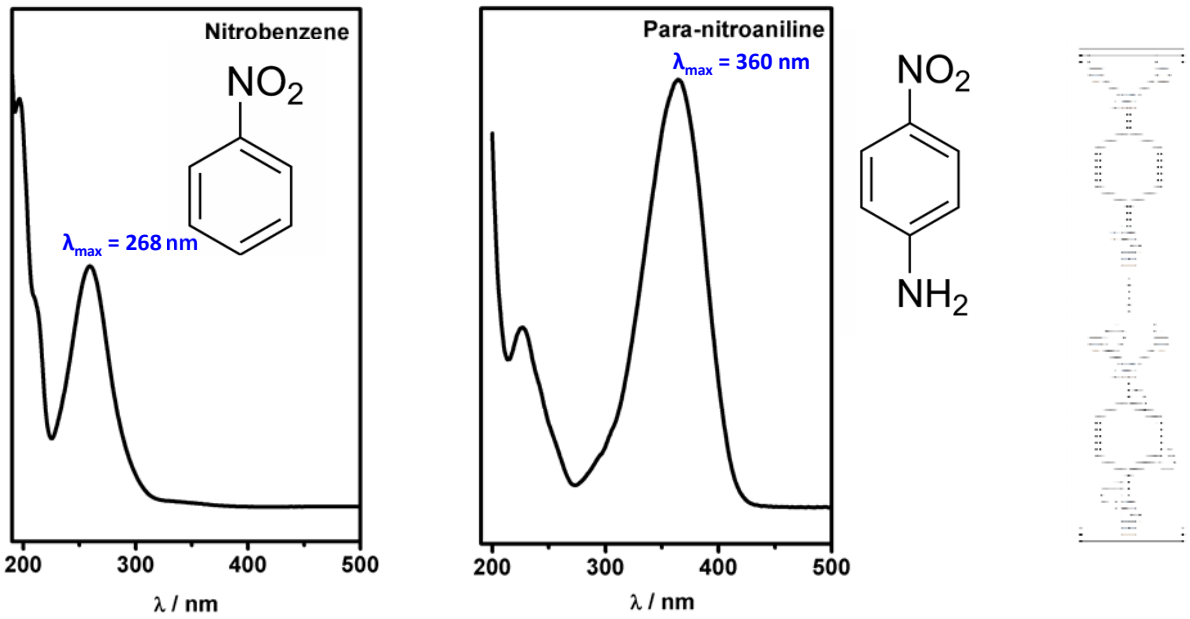

Aromáticos

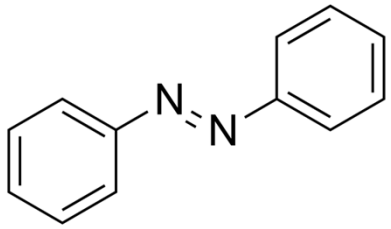

Ex: azobenzene

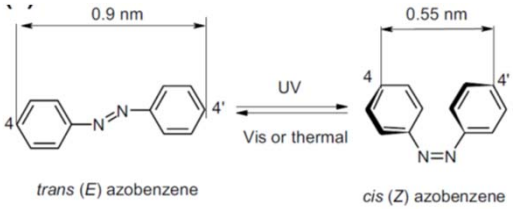

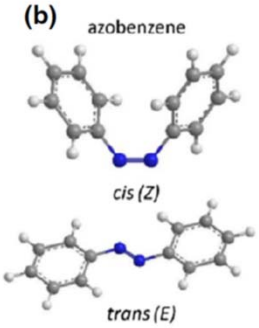

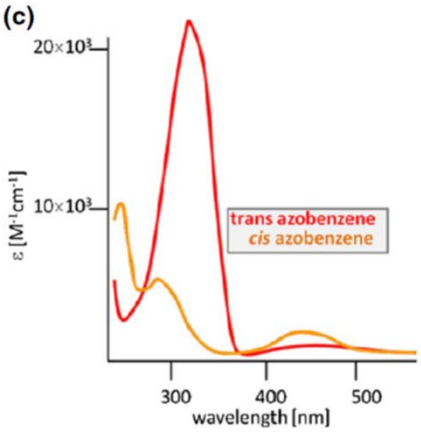

Wysiecka W. et al. Journal of Inclusion Phenomena 90 (2018) 189–257

Aromáticos – Corantes AZO

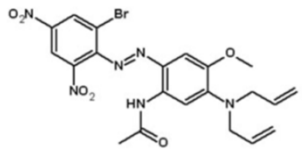

Disperse Blue 373

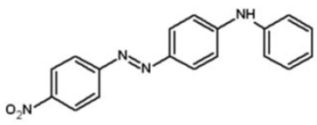

Disperse Orange 1

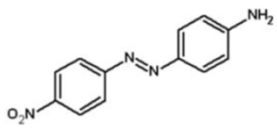

Disperse Orange 3

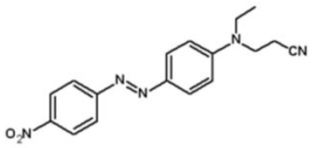

Disperse Orange 25

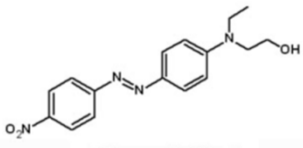

Disperse Red 1

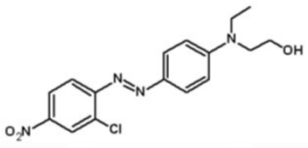

Disperse Red 13

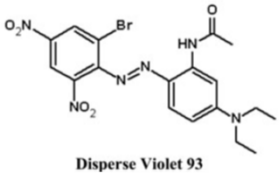

Disperse Violet 93

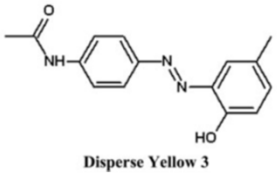

Disperse Yellow 3

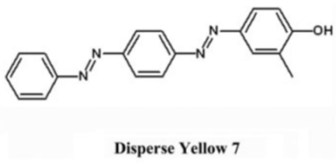

Disperse Yellow 7

Zocolo G. J. et al. Journal of Chromatographic Science (2015) 1-8

685 pages

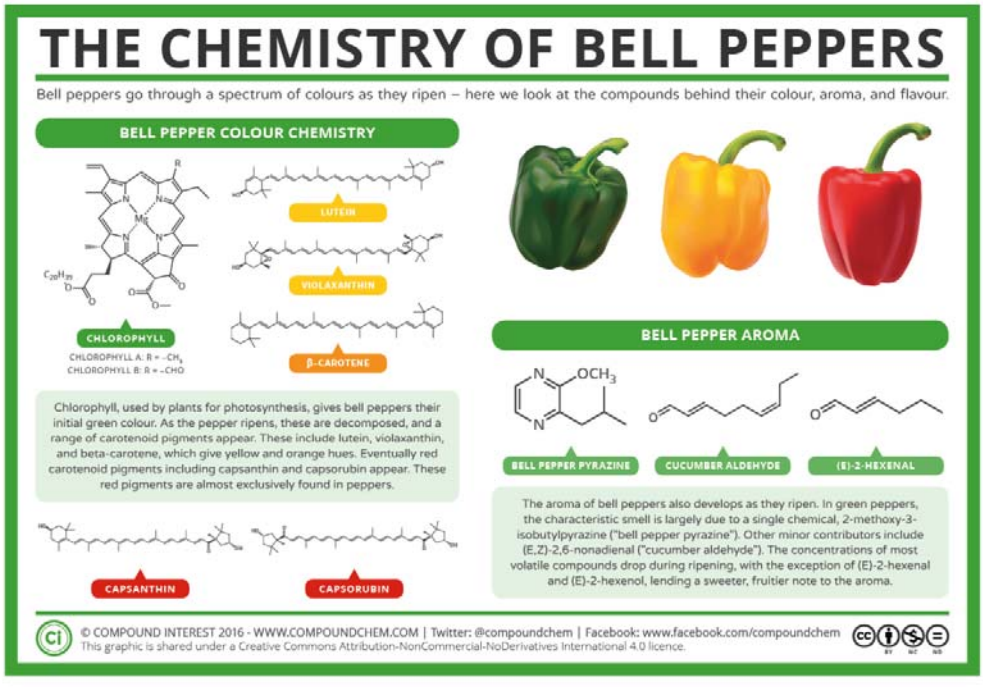

Aromáticos – Antocianinas

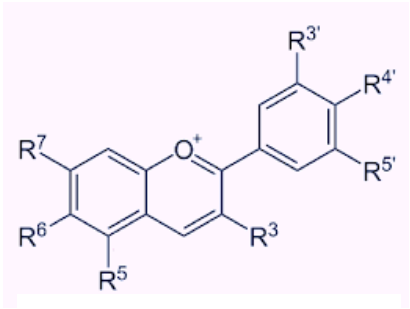

Tena N. et al. Antioxidants 9 (2020) 451–257

Efeito da conjugação

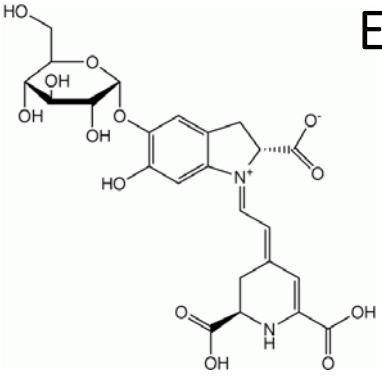

Ex: betanine

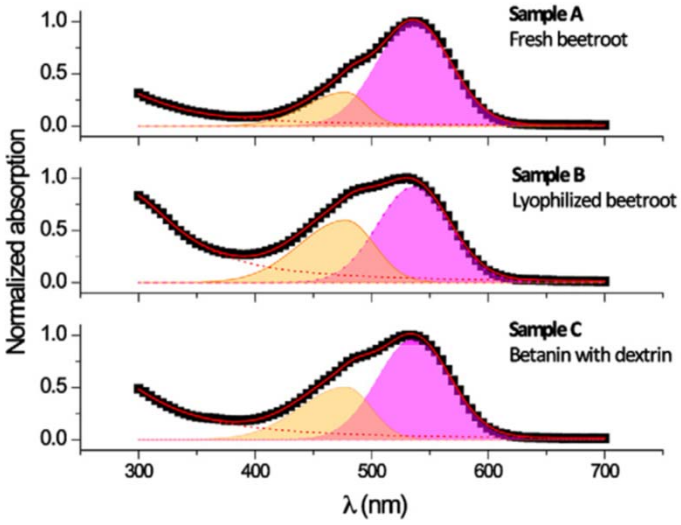

Bastos E. L. et al. Food Chemistry 131 (2012) 231–238

Beetblue

SHARE

RESEARCH ARTICLE | CHEMISTRY

A metal-free blue chromophore derived from plant pigments

B. C. Freitas-Dörr[1], C. O. Machado[1], A. C. Pinheiro[1], A. B. Fernandes[1], F. A. Dörr[2], E. Pinto[2], M. Lopes-Ferreira[3], M. Abdellah[4,5], J. Sá[4,6], L. C. Russo[7], F. L. Forti[7], L. C. P. Gonçalves[1] and E. L. Bastos[1,*]

[1]Departamento de Química Fundamental, Instituto de Química, Universidade de São Paulo, 05508-000 São Paulo, SP, Brazil.

[2]Departamento de Análises Clínicas e Toxicológicas, Faculdade de Ciências Farmacêuticas, Universidade de São Paulo, 05508-000 São Paulo, SP, Brazil.

[3]Immunoregulation Unit of the Special Laboratory of Applied Toxinology (Center for Toxins, Immune-Response and Cell Signaling/CEPID/FAPESP), Butantan Institute, 05503-900 São Paulo, SP, Brazil.

[4]Physical Chemistry Division, Department of Chemistry, Ångström Laboratory, Uppsala University, 75120 Uppsala, Sweden.

[5]Department of Chemistry, Qena Faculty of Science, South Valley University, 83523 Qena, Egypt.

[6]Institute of Physical Chemistry, Polish Academy of Sciences, 01-224 Warsaw, Poland.

[7]Departamento de Bioquímica, Instituto de Química, Universidade de São Paulo, 05508-000 São Paulo, SP, Brazil.

*Corresponding author. Email: elbastos@iq.usp.br

Hide authors and affiliations

Science Advances 03 Apr 2020:
Vol. 6, no. 14, eaaz0421
DOI: 10.1126/sciadv.aaz0421

Beetblue

Universidade de São Paulo
Instituto de Química

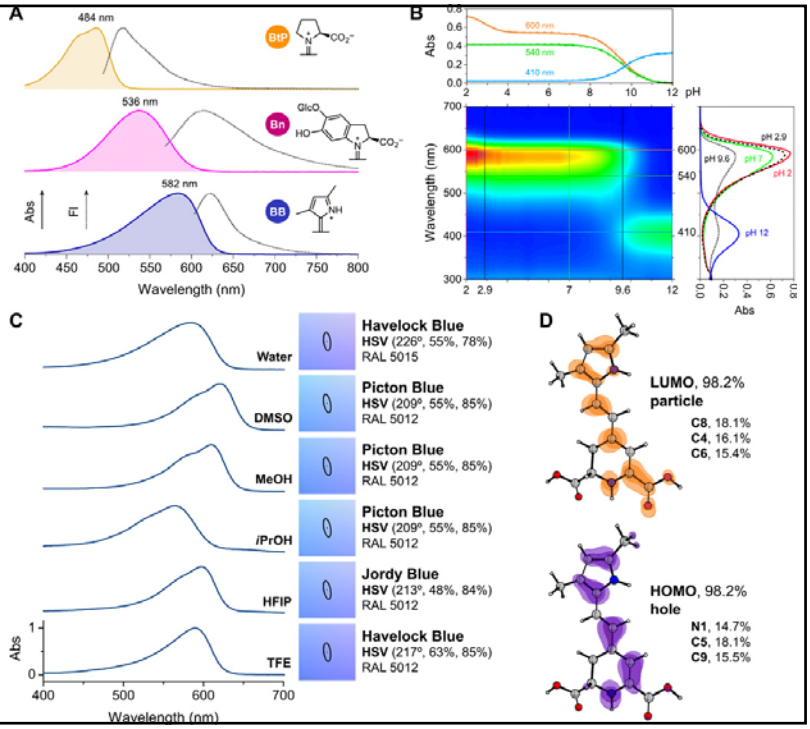

Bastos E. L. et al. Science Advances 6 (2020) 1–7

Aromáticos – Corantes Solvatocromicos

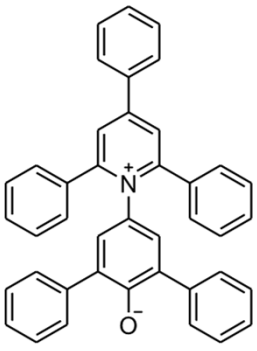

Ex: Reichardt`s betaine

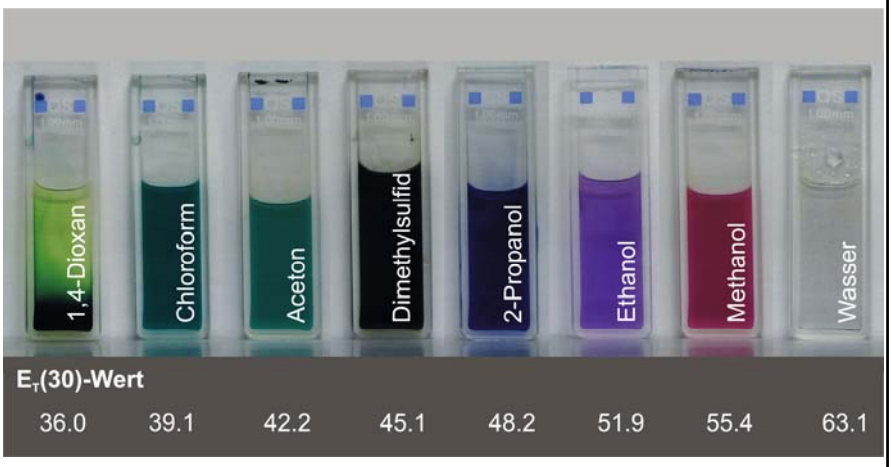

Diagrama de Jablonski

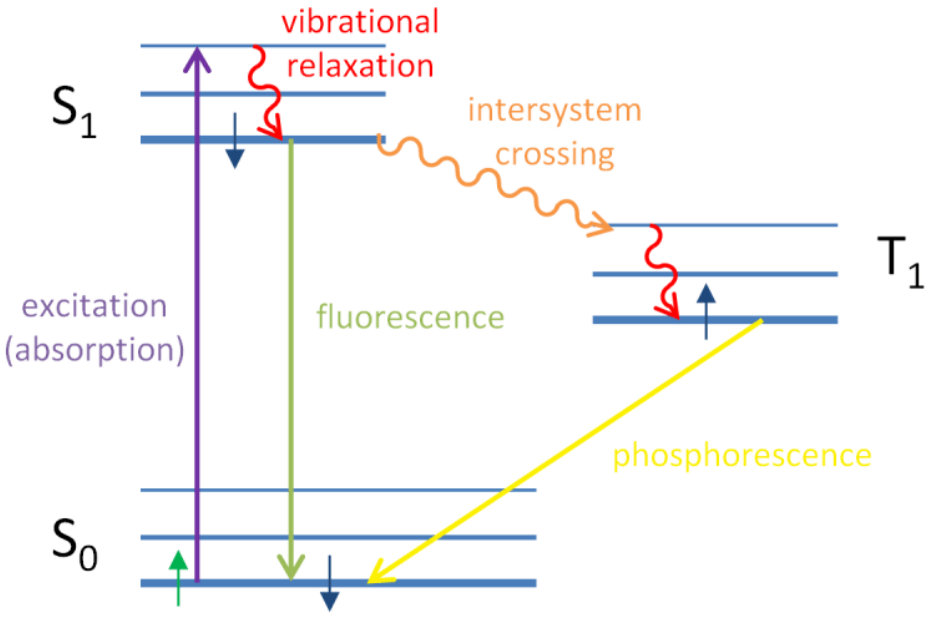

Níveis de energia e transições

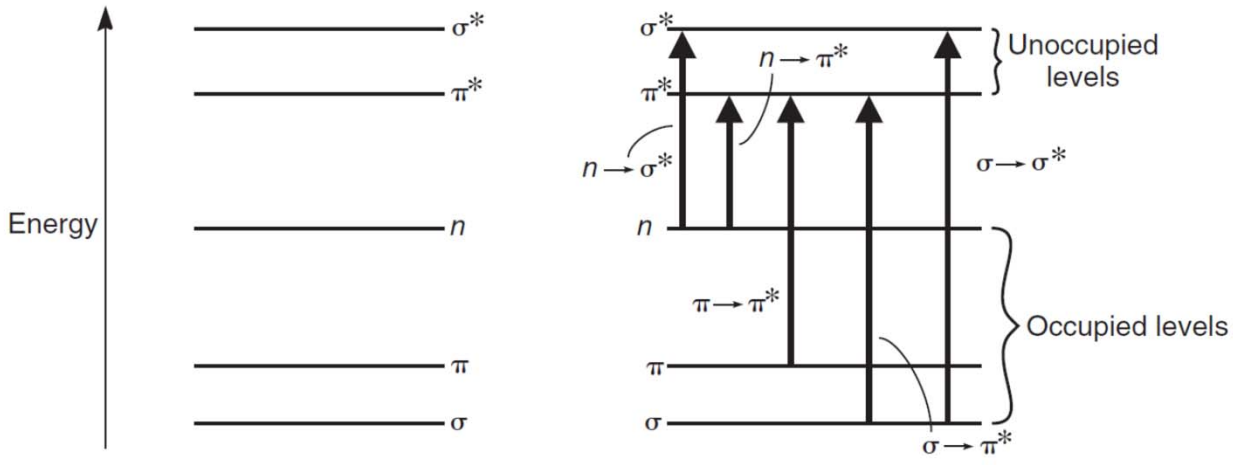

Exemplos de transições em compostos orgânicos

Increasing energy

$\sigma \longrightarrow \sigma^*$	In alkanes
$\sigma \longrightarrow \pi^*$	In carbonyl compounds
$\pi \longrightarrow \pi^*$	In alkenes, carbonyl compounds, alkynes, azo compounds, and so on
$n \longrightarrow \sigma^*$	In oxygen, nitrogen, sulfur, and halogen compounds
$n \longrightarrow \pi^*$	In carbonyl compounds

Alcanos

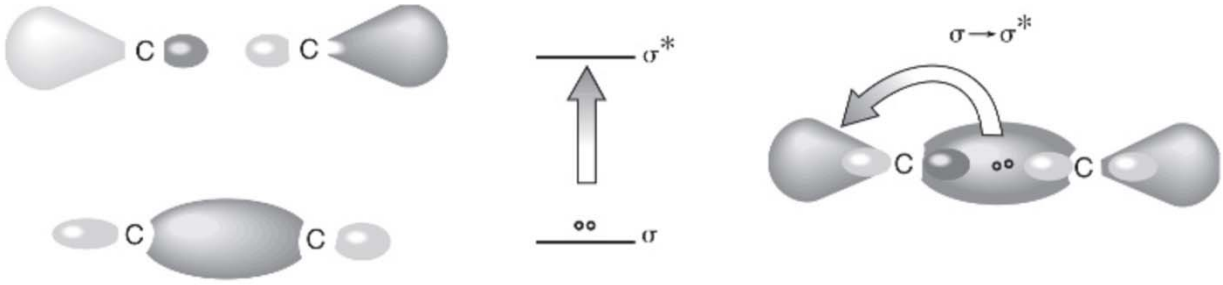

Alcenos

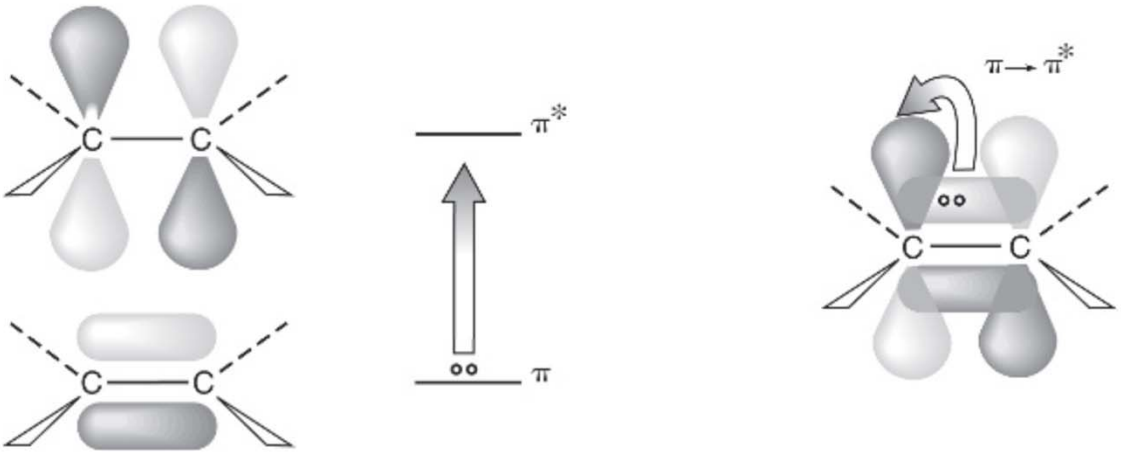

Aminas

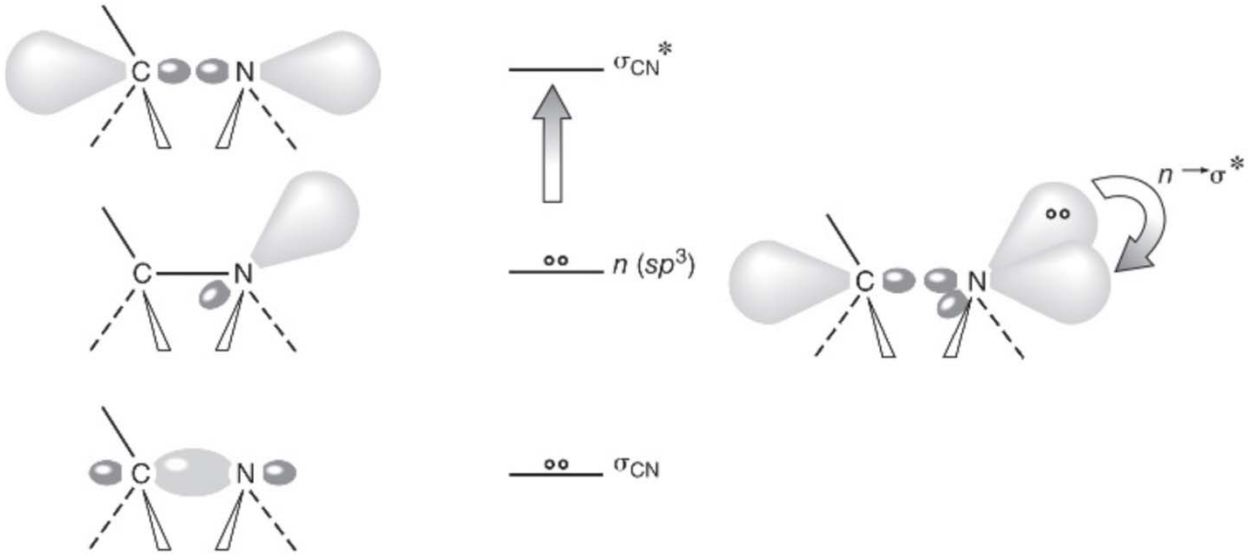

Compostos carbonílicos

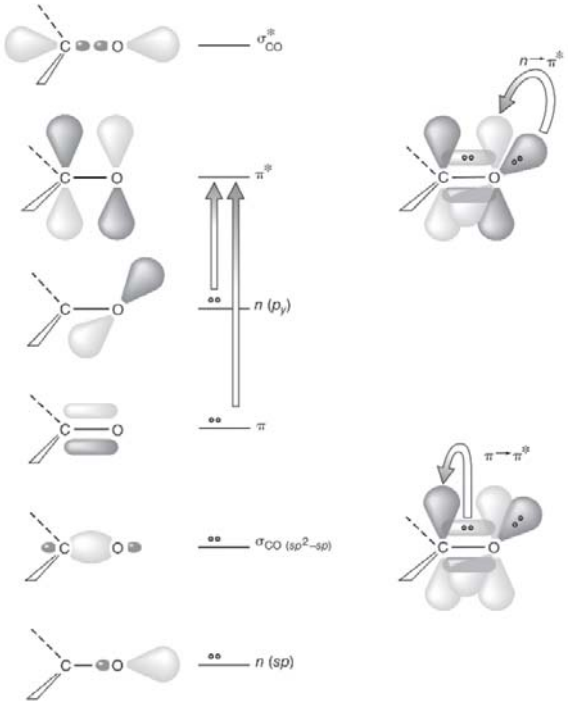

Cromóforos

TYPICAL ABSORPTIONS OF SIMPLE ISOLATED CHROMOPHORES

Class	Transition	λ_{max} (nm)	log ε	Class	Transition	λ_{max} (nm)	log ε
R−OH	$n \rightarrow \sigma^*$	180	2.5	$R-NO_2$	$n \rightarrow \pi^*$	271	<1.0
R−O−R	$n \rightarrow \sigma^*$	180	3.5	R−CHO	$\pi \rightarrow \pi^*$	190	2.0
$R-NH_2$	$n \rightarrow \sigma^*$	190	3.5		$n \rightarrow \pi^*$	290	1.0
R−SH	$n \rightarrow \sigma^*$	210	3.0	R_2CO	$\pi \rightarrow \pi^*$	180	3.0
$R_2C{=}CR_2$	$\pi \rightarrow \pi^*$	175	3.0		$n \rightarrow \pi^*$	280	1.5
R−C≡C−R	$\pi \rightarrow \pi^*$	170	3.0	RCOOH	$n \rightarrow \pi^*$	205	1.5
R−C≡N	$n \rightarrow \pi^*$	160	<1.0	RCOOR′	$n \rightarrow \pi^*$	205	1.5
R−N=N−R	$n \rightarrow \pi^*$	340	<1.0	$RCONH_2$	$n \rightarrow \pi^*$	210	1.5

Dependência com o solvente

Ex: acetone

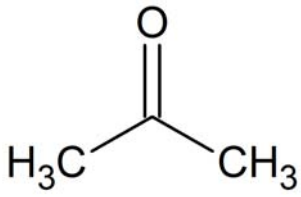

Solvent	λ_{max} ($n \rightarrow \pi^*$) / nm
Water, H_2O	264
Methanol, CH_3OH	270
Ethanol, CH_3CH_2OH	272
Chloroform, $CHCl_3$	277
Hexane, C_6H_{14}	279

Dependência com o solvente

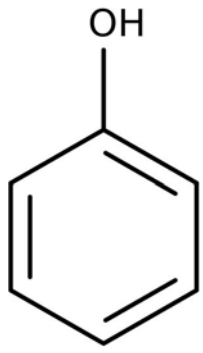

Ex: phenol

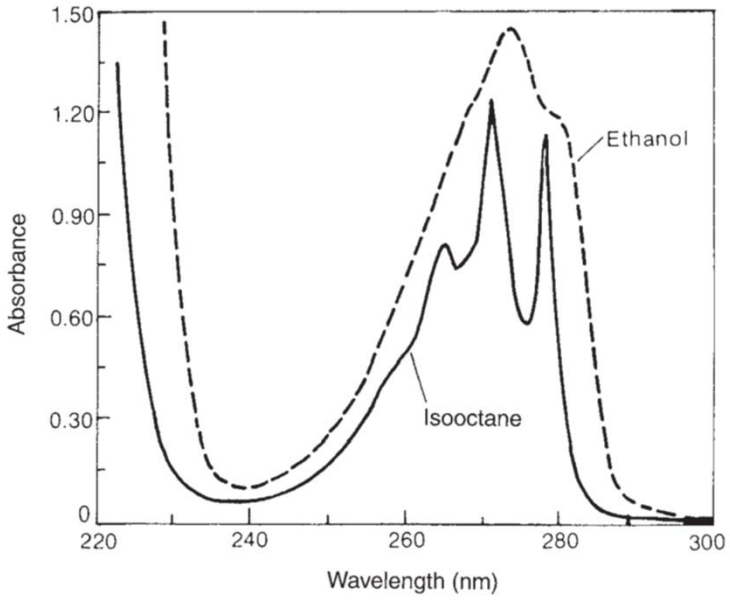

Efeito da conjugação

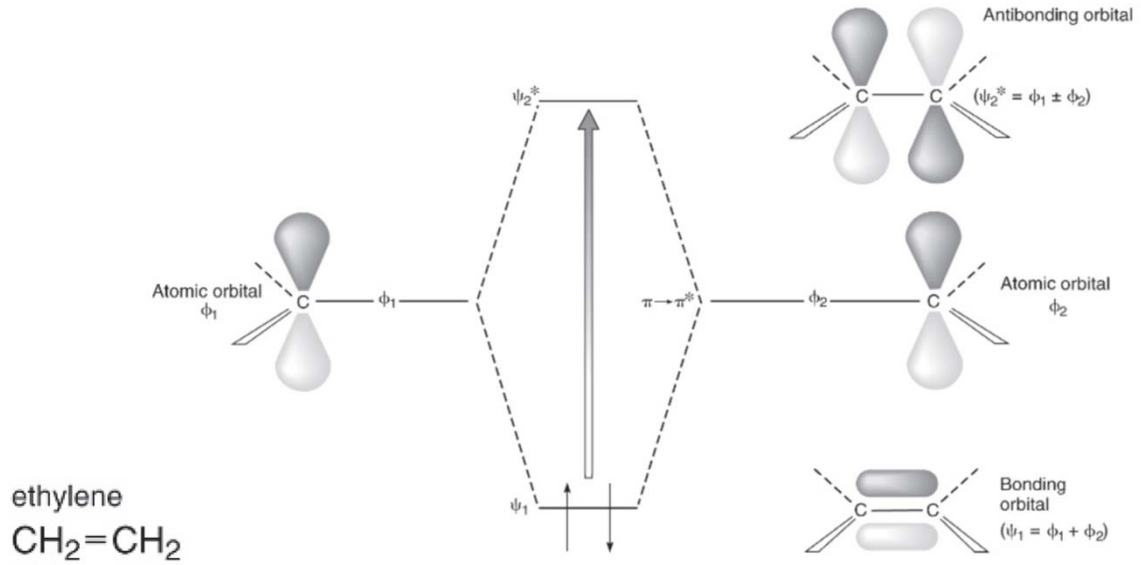

Efeito da conjugação

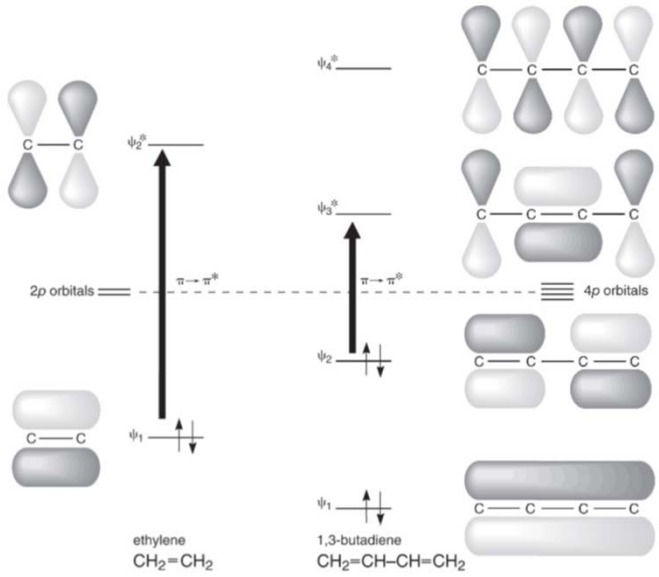

Aromáticos

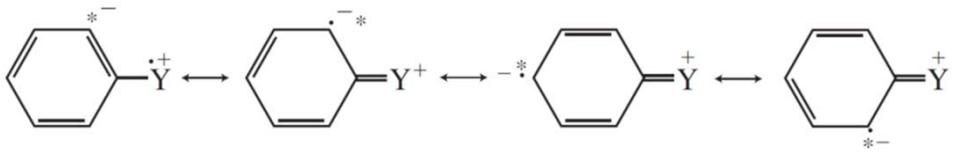

pH EFFECTS ON ABSORPTION BANDS

Substituent	Primary λ (nm)	Primary ε	Secondary λ (nm)	Secondary ε
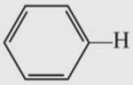	203.5	7,400	254	204
—OH	210.5	6,200	270	1,450
$-O^-$	235	9,400	287	2,600
$-NH_2$	230	8,600	280	1,430
$-NH_3^+$	203	7,500	254	169
—COOH	230	11,600	273	970
$-COO^-$	224	8,700	268	560

Aromáticos

ULTRAVIOLET MAXIMA FOR VARIOUS AROMATIC COMPOUNDS

Substituent		Primary λ (nm)	Primary ε	Secondary λ (nm)	Secondary ε
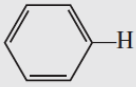		203.5	7,400	254	204
Electron-releasing substituents	$-CH_3$	206.5	7,000	261	225
	—Cl	209.5	7,400	263.5	190
	—Br	210	7,900	261	192
	—OH	210.5	6,200	270	1,450
	$-OCH_3$	217	6,400	269	1,480
	$-NH_2$	230	8,600	280	1,430
Electron-withdrawing substituents	—CN	224	13,000	271	1,000
	—COOH	230	11,600	273	970
	$-COCH_3$	245.5	9,800		
	—CHO	249.5	11,400		
	$-NO_2$	268.5	7,800		